6-18-2009

# Software Automation For Measurement-Based Behavioral Models Of Microwave

Daniel Sosa Martin
*University of South Florida*

# Software Automation For Measurement-Based Behavioral Models Of Microwave Amplifiers

by

Daniel Sosa Martin

A thesis submitted in partial fulfillment
of the requirements for the degree of
Master of Science in Electrical Engineering
Department of Electrical Engineering
College of Engineering
University of South Florida

Co-Major Professor: Lawrence P. Dunleavy, Ph.D.
Co-Major Professor: Jing Wang, Ph.D.
Thomas M. Weller, Ph.D.

Date of Approval:
June 18, 2009

Keywords: rf, measurement, behavioral model, non linear, power amplifier, s-parameter, network analyzer

**ACKNOWLEDGEMENTS**

I would like to thank Dr. Lawrence Dunleavy for giving me the opportunity to work in his research group. I would also like to thank Dr. Thomas Weller for his good teachings and for reviewing my work.

I would like to thank Modelithics, Inc. for directly funding my research work. Thank you also to Rick Connick who participated in the origins of this work and with whom I developed some of the measurement procedures presented here.

Many thanks to Dr. Jon Martens from Anritsu for his help with the development and troubleshooting of the HOT S-Parameter measurement setup. To Dr. Joel Dunsmore from Agilent who pointed out some details to consider with power sweep measurements. To Tom Le from Agilent support who clarified some components in the P2D model. To Rick Morehouse from Anritsu support who proposed the methodology used to measure all the power levels set with the Anritsu Lightning VNA.

To Alberto Rodriguez, for his early teachings on RF measurement, VNA calibration, and LabVIEW programming. Thank you to past and present friends in ENB 412 for their help and for sharing all the good and bad times that university imply.

Finally, I would like to thank my mother Maria del Carmen, aunt Mercedes, uncle Agustin, and grandmother Mercedes for all their support and encouragement through all my life, and without whom I would have never got this far.

## TABLE OF CONTENTS

## LIST OF TABLES

## LIST OF FIGURES

**Software Automation for Measurement-Based Behavioral Models of Microwave Amplifiers**

Daniel Sosa Martin

## ABSTRACT

This thesis presents a study and implementation of several measurement procedures used to efficiently generate non-linear measurement-based behavioral models primary for microwave amplifiers. Behavioral models are a solution for representing devices that can present linear and/or non-linear behavior when little or no information about the internal structure is known. Measurement-based behavioral models are an advantage since they can be extracted from a direct measurement of the device. This work addresses some of the challenges of these types of measurements. A set of software modules has been produced that combine several modern techniques to efficiently generate practical models using equipment commonly available in a typical microwave lab. Advanced models using new and more complex equipment are also discussed.

Modeling of the non-linear operation of power amplifiers is a common subject of study since it provides a path to improved system simulations. However, the measurement process used for non-linear behavioral modeling of PAs requires either non-linear measurement instrumentation, not yet widely available, or numerous measurements that makes the process tedious and susceptible to errors. Power dependent

S-Parameters obtained with a conventional Vector Network Analyzers (VNA) can be used to extract AM-to-AM and AM-to-PM behavior of a device and to generate, simple but useful, behavioral models. A careful analysis of the characteristics of common RF measurement instrumentation combined with knowledge of common non-linear phenomena provides with the conditions under which useful models can be generated.

The results of this work are presented as several programs implemented in National Instruments LabVIEW that will sequence through the different measurements required for the generation of measurement-based behavioral models. The implemented models are known as P2D and S2D models available with Agilent Advanced Design System (ADS.) The code will communicate with the measurement instrumentation and decide on the most efficient way to extract the data. Once the data is extracted, the code will put into the appropriate syntaxes required by the model for direct and convenient setup of the generated models in ADS.

# CHAPTER 1

# INTRODUCTION

## 1.1 Background and Motivation

The use of simulation software in electronic engineering design is the common practice nowadays. A simulator can provide a significant reduction in time and cost of the implementation of any electronic system. Provided adequate models are available for system elements, simulators can accurately predict the response of a system allowing the engineer to tune the design to obtain the desired response before fabrication. In order to be able to predict the response of a system, the simulator must have accurate models of all the elements that compose it. Therefore, the generation of accurate simulation models plays an important role in modern electronic design. In particular, this work focuses on measurement based behavioral models for microwave amplifiers.

Traditional circuit model generation requires direct measurements of the device combined with a certain a priori knowledge of its physical structure. Two aspects make this process considerably challenging: frequency and non-linear response. An increase in frequency increases the complexity of the model as it will have to account for parasitic and/or electromagnetic effects. The inclusion of such effects in the model will require a more detailed knowledge of the device and often results in larger simulation times. On the other hand, when the device is intended to be modeled under non-linear conditions it

will not only add more complexity to the model, but also require the use of expensive measurement instrumentation and more involved measurements. The purpose of this thesis is to provide a solution to generate high frequency non-linear models using a time efficient approach with readably available measurement instrumentation.

Behavioral models will be used for the proposed solution as they do not require detailed information of the device's internal structure and they will reduce simulation time with respect to other types of models. Measurement based behavioral models were selected for this work as they can be directly generated from measurements of the device. The price of this simplification will be a multiplication of the total number of measurements needed to generate the model, as the device will have to be measured over the range of conditions under which it needs to be modeled. Additional measurements are also required for non linear behavior which depending on the instrumentation available and model approach may imply significant additional effort. In order to overcome these laborious measurements, an analysis of the capabilities of network analyzers and implementation of code used to control them and automate the measurement is achieved and demonstrated.

### 1.2 Contribution of the Thesis

This thesis presents an analysis of the existing methods used for obtaining non-linear measurements with network analyzers and combines at least two of these methods to apply them to behavioral model generation. With this analysis a measurement procedure and automation implemented as a LabVIEW application was developed. This application demonstrated a significant reduction in the total time needed for the

generation of the model. The example presented in Chapter 5 showed an increase in the time efficiency of more than 500% with software automation compared to a manual procedure.

### 1.3 Organization

This thesis is organized into four main chapters using the following structure.

- Chapter 2 will present a literature review of behavioral modeling theory with an emphasis on measurement based models. This chapter will describe most commonly studied measurement-based behavioral models and common methods used to generate them. Some concepts of non linear system theory are also summarized as they apply to modeling theory.
- Chapter 3 will summarize typical implementation for linear and non linear measurements with network analyzers. S-parameter calibration, AM-to-AM, AM-to-PM, HOT S-parameters and the new Agilent PhD model are the topics covered.
- Chapter 4 first states the particular problem to be solved in terms of the model to generate, the instrumentation to use, and issues like calibration and time efficiency. It presents an analysis of the instrumentation and how the process can be made more efficient. Finally, it lists the algorithms proposed to automate the process of generating S2D and P2D types of models.
- Chapter 5 demonstrates the implemented methods and code with commercial amplifiers.
- Chapter 6 summarizes all the work presented and proposed some lines for future development.

# CHAPTER 2

# GENERAL THEORY OF BEHAVIORAL MODELING

This Chapter presents an overview of behavioral modeling for microwave amplifiers. Some of the most popular behavioral models are introduced with an emphasis on those relevant to the work presented herein.

## 2.1 Introduction to Behavioral Modeling

In modern circuit simulation tools three kinds of device models are commonly used: physical models, circuit models, and behavioral models. The previous classification is ordered by level of abstraction. A physical model will describe the characteristics of the device from the most elemental physical principles and will include all the fabrication characteristics of the device. Circuit models use a circuit network whose elements can be associated with the different electrical phenomena occurring in the device. Finally, behavioral models relate the possible responses of the device with the excitation that originated them. These three different approaches have different levels of performance, accuracy, and complexity. In this way, physical models will be able to predict the performance of the device under a wider set of conditions but will also require higher computing capabilities and a detailed knowledge of the device's internal construction. On the other hand, behavioral models can be generated with minimum a priori information of

the device but require extensive and advance equipment and methods to characterize non-linear behavior. Circuit models are an intermediate stage between behavioral and physical models.

While physical and circuit models need the simulator to solve networks (circuits) and/or geometric meshes (electromagnetism,) behavioral models map inputs (excitations) with outputs (responses.) The fact that no detailed information about the device is assumed makes it commonly named as 'Black-Box' models.


**Figure 2.1 - Behavioral Modeling Approach**

The different ways behavioral models relate inputs to outputs are used here to classify the different possible behavioral models into the following categories:

- Parametric/Parameterized. These models are described using some of the typical fundamental characteristic of electrical systems like gain, bandwidth, gain compression, intermodulation distortion, noise figure, etc… The simulator will use, through the appropriate mathematical descriptions, these parameters to estimate the response of the device.
- Equation based. These models mathematically relate inputs to outputs with an equation. In general, different models will use different equations and they will differ in a set of coefficients to be applied to the equation. Equation based models are similar in nature to the parametric based models; however, parametric based models will most commonly use typical figures of merit of the device rather than

mathematical coefficients. Some of the more common equation based models are listed below:

- Polynomials. These models use a power series to describe linear and non-linear characteristic of the device. The coefficients of the polynomial can be obtained through fitting or optimization.
- Volterra Series. A Volterra series are functional series that will represent a system (linear or non-linear) with a multidimensional convolution operation [1]. The terms that model the system are known as kernels and can be used to represent non-linear response and memory effects, as well. Volterra series provide high accuracy with the disadvantage of high computation requirements.

- Measurement based. Measurement based models are those which map inputs to outputs based on a set of measurements. The goal is to obtain enough data points under different measurement conditions (excitation, bias, temperature) so the response of the device to an excitation can be directly connected to one of the measurements. When data is not available for every modeling condition, interpolation and/or other techniques can be used obtain the response of the model. Some examples of measurement based models are listed below.
  - Simple measurement files. A simple file containing S-Parameters or any other network parameters (Z, Y, ABCD) can be considered as a behavioral model. The limitation of these files is that they model the behavior only under liner conditions.

- P2D models. P2D are Agilent ADS [2] built-in models. They contain multiple sets of network parameters (e.g. S-Parameters) measured under linear (frequency swept) and non-linear (power swept) conditions. These models can predict the effects caused by S-parameter dependence on power (e.g. gain compression and spectral regrow) but limited only to the fundamental frequency response.
- S2D models. S2D are also Agilent ADS [2] built-in models and they have a similar structure than P2D. The difference between P2D and S2D is the way in which the non-linear block is stored and used. S2D models require only $S_{21}$ data normalized for magnitude and phase versus power. This data will be used during the simulation to perform an odd order polynomial fitting [3] that will enable the simulator to predict odd order harmonics and intermodulation products [3-4] but not even order effects.
- Poly Harmonic Distortion (PHD) Model. The PHD model is a natural extension of the S-Parameters [5] to characterize non-linear networks. The main difference with classical S-parameters is the ability to relate an input at a fundamental frequency to multiple frequency outputs. In order to generate this model a Large Signal Network Analyzer (LSNA) is required.
- A simplified PHD model. This model has the same structure as the PHD model but it can be generated with classical VNAs when it is reasonable to approximate $S_{12}=0$. The model can be generated with a load pull setup where S-parameters with multiple load impedance are measured, and

through a fitting process the coefficients required for the PHD model will be calculated [6].

The general classification of the different behavioral models is further illustrated in Figure 2.2.

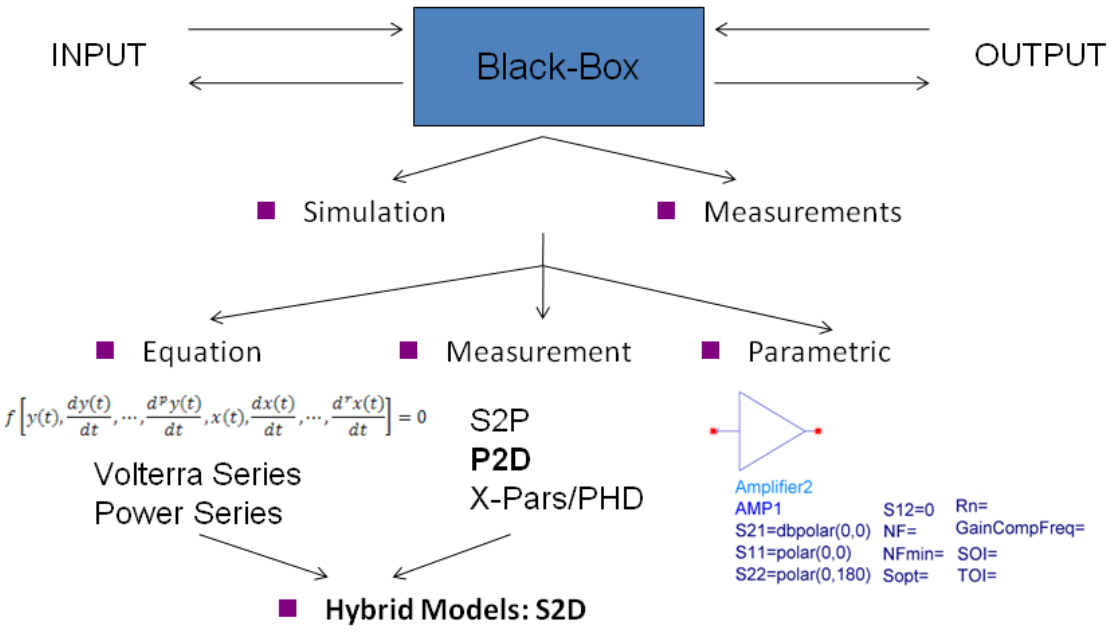


**Figure 2.2 - Classification of Behavioral Models**

Some of the advantages introduced by behavioral modeling are listed below:

- Protects intellectual property. Since the extraction of the model does not require any knowledge of the device itself, the modeling can be done without giving out proprietary designs.
- Speeds up simulation. A behavioral model will predict the response of a device faster than a classical circuit or physical model. Especially when the device is composed of multiple subsystems the simulation can be time consuming.

- In those cases, where the response of the device does not fit well to any available circuit and/or physical models behavioral models can be a practical and faster solution to implement.

## 2.2 Non-linear Systems

Homogeneity and superposition are the two properties that classify a system as linear. These two properties imply that given a combination of excitations $x_1(t)+x_2(t)+..+x_n(t)$ input to a linear system, the response will be composed of the summation of the individual responses to the input excitations.


**Figure 2.3 – Linear System**

Any system that does not meet the conditions of superposition and homogeneity is considered non-linear and will present additional characteristics that make its response more difficult to predict. Below, we present some of those characteristics. For simplicity, we will use a simple power series to represent a generic nonlinear system. This representation is appropriate since it will give an insight of the most common effects of non-linear response. For the rest of this chapter we will consider a system with the following response:

$$y(t) = K_1 \cdot x(t) + K_2 \cdot x^2(t) + K_3 \cdot x^3(t) \qquad (1.1)$$

and we will use one or several sinusoidal excitations as it is common in circuit theory.

$$x(t) = A \cdot \cos(w_1 \cdot t) + B \cdot \cos(w_2 \cdot t) \qquad (1.2)$$

### 2.2.1 Harmonic Generation

For a given one tone excitation:

$$x(t) = A \cdot \cos(w_1 \cdot t) \tag{1.3}$$

the response of a non linear system will be

$$\begin{aligned} y(t) &= K_1 \cdot A \cdot \cos(w_1 \cdot t) + K_2 \cdot \left(A \cdot \cos(w_1 \cdot t)\right)^2 \\ &\quad + K_3 \cdot \left(A \cdot \cos(w_1 \cdot t)\right)^3 \\ &= \frac{K_2 \cdot A^2}{2} + \left( K_1 \cdot A + \frac{3 \cdot K_3 \cdot A^3}{4} \right) \cdot \cos(w \cdot t) \\ &\quad + \frac{K_2 \cdot A^2}{2} \cos(2wt) + \frac{K_3 \cdot A^3}{4} \cos(3w \cdot t) \end{aligned} \tag{1.4}$$

From equation (4) we can see how from a single input frequency, a non linear system will generate additional frequencies at multiples of the input. The new frequencies are harmonics and they are of significant importance in broadband systems. As we can see the amount of energy delivered to the harmonic frequencies will depend on the level of non linearity, which for the power series representation used in (1), depends on the values of the $K_2$ and $K_3$ coefficients. In addition, combinations of multiple non-linear devices result in harmonic levels that depend on the phase and amplitudes of each individual device's harmonic response.

### 2.2.2 Gain Conversion (AM-to-AM)

In equation (1) we can see that apart from the effect of harmonic generation, the coefficient corresponding to the third order non linearity of the system ($K_3$) will modify the amplitude of the fundamental frequency by a factor equal to the cube of the amplitude of the excitation ($A^3$). This effect is commonly known as the AM to AM characteristic of

the system and when the $K_3$ coefficient is negative, which is the usual case, it is also called gain compression. Gain compression implies a reduction in the gain of the system as the signal level at its input increases.

### 2.2.3 Phase Conversion (AM-to-PM)

A similar effect can be found with the phase response of the systems. An example system that will present AM-to-PM conversion effects will have the following response to the same excitation shown in equation (1.3).

$$y(t) = \frac{K_2 \cdot A^2}{2} + \left( K_1 \cdot A + \frac{3 \cdot K_3 \cdot A^3}{4} \cdot e^{j\varphi} \right) \cdot \cos(w \cdot t) + \ldots \qquad (1.5)$$

As we can see, the term is now multiplied by an exponentional that will shift the phase of the cosine function. In the same manner as with AM-to-AM the shift in phase will be weighted by the cube of the amplitude of the excitation. The consequence will be a change in phase in the fundamental output as a function of the input power level.

### 2.2.4 Intermodulation Distortion

When the excitation to a system contains multiple frequency components the non-linear response will generate additional frequency products that need further consideration. To illustrate this, let's use a two tone signal of the form presented on at equation (1.2) as the input to the non-linear system represented by equation (1.1).

$$
\begin{aligned}
y(t) &= K_1 \cdot (A \cdot \cos(w_1 \cdot t) + B \cdot \cos(w_2 \cdot t)) + K_2 \cdot (A \cdot \cos(w_1 \cdot t) + B \cdot \cos(w_2 \cdot t))^2 \\
&\quad + K_3 \cdot (A \cdot \cos(w_1 \cdot t) + B \cdot \cos(w_2 \cdot t))^3 \\
&= K_1 \cdot A \cdot \cos(w_1 \cdot t) + K_1 \cdot B \cdot \cos(w_2 \cdot t) + \frac{K_2}{2} A_1^2 + \frac{K_2}{2} A_2^2 + \frac{K_2}{2} A^2 \cos(2w_1 t) \\
&\quad + \frac{K_2}{2} B^2 \cos(2w_2 t) + \frac{K_2}{2} \cdot 2 \cdot A \cdot B \cdot \cos((w_1 + w_2) \cdot t) \\
&\quad + \frac{K_2}{2} \cdot 2 \cdot A \cdot B \cdot \cos((w_1 - w_2) \cdot t) + \frac{K_3}{4} A^3 \cos(3w_1 t) \\
&\quad + \frac{K_3}{4} B^3 \cos(3w_1 t) + \frac{K_3}{4} 3 \cdot A^2 B \cos((2w_1 + w_2)t) \\
&\quad + \frac{K_3}{4} 3 \cdot A^2 B \cos((2w_1 - w_2)t) + \frac{K_3}{4} 3 \cdot A B^2 \cos((w_1 + 2w_2)t) \\
&\quad + \frac{K_3}{4} 3 \cdot A B^2 \cos((w_1 - 2w_2)t) + \frac{K_3}{4} (A^3 + 2AB^2) \cdot \cos(w_1 t) \\
&\quad + \frac{K_3}{4} (B^3 + 2A^2 B) \cdot \cos(w_1 t)
\end{aligned} \tag{1.6}
$$

From the previous development we can distinguish how several new frequency terms have been generated. Those new terms multiples of the two input frequencies and are usually named as intermodulation products. Given an intermodulation product the order of the product will be n+m.

In narrowband amplifiers with multiple excitations most of the higher intermodulation frequency products will be filtered out by the different matching stages of the amplifier. However, when the two input frequencies are close, the difference in frequency between odd order products and the inputs will be small and difficult to discriminate. The odd order products can be therefore a major cause of distortion that will translate into some common problems in communication systems like adjacent-channel interference.

The third order intermodulation product is the one of most concern since its power grows rapidly with nonlinearity. The third order intercept point (IP3) is frequently

used as a figure of merit of a system, and it is defined as the intercept point between the line whose slope is the coefficient of the linear component and the line whose slope is the coefficient of the third order intermodulation product.

### 2.2.5 Memory Effects

Memory effects can be defined as differences in the behavior of a device under dynamic and static conditions and are classified as non linear behavior. Causes of memory effects are [7, 8]:

- Dynamic thermal effects;
- Unintentional modulation on supply rails;
- Semiconductor trapping effects;
- Long time constants in dc-bias networks.

Memory effects are more significant in RF power amplifiers, where it is common to operate at higher levels of non linearity, and where the use of modulated signal may be more affected by this type of distortion. Memory effects can be sub classified into short term and long term depending on whether their time constant is on the order of the carrier or the envelope period of the signal [8].

One of the most common manifestations of memory effects is asymmetries in the intermodulation side bands [9]. These asymmetries are a consequence of a time lag between the AM-to-AM and AM-to-PM responses at the test frequency [10].

### 2.2.6 Non-linear Effects in Communication Systems

The importance of the previously mentioned effects arises when non linear devices (e.g. RF power amplifiers, mixers) are present in communication systems. The non-linear response will translate into distortion that may produce errors in the communication or even make it impossible at all. Most significant effects of non-linear response are listed below [11]:

- Adjacent Channel Interference. As other frequencies like harmonics and intermodulation products are generated, the frequency bands assigned to other communication channels can be invaded. This situation will degrade the quality of the communication link. This effect is also commonly known as spectral regrowth, and co-channel interference.
- Cross Modulation. This effect appears when a modulated signal transfers its modulation to other frequencies present in the system.
- Spurious responses. Mixers will generate additional frequencies other than the corresponding mixing products. Depending on the input power the number of additional generated frequencies will vary.

The previous list adds to advantages of generating non-linear models as they can predict undesired responses in a communication system and be used to mitigate them.

## 2.3 Parametric Behavioral Models

Parametric based behavioral models are based on different factors of system performance. These factors represent some of the usual characteristics of linear and non linear systems including gain, noise figure, 1dB compression point, intermodulation intercept point (e.g IP3 and IP5). Once the parameters have been defined the simulator should apply the appropriate math to use those parameters in the simulation.

## 2.4 Equation Based Behavioral Models

Equation based behavioral models will fit a set of coefficients to an equation that mathematically describes the response of the system. Equation based models differ from parametric based models in that the coefficients will not have any physical meaning.

### 2.4.1 Classical Equation Based Models

A good overview of classical behavioral models is presented in [12] by Maas and Pedro. In [12] a classification of behavioral models is made based on the memory of the system to be modeled. This classification is summarized below.

- Memoryless models. These models assume an instant change in the output envelope of a modulated signal with changes at the input and can be understood as a simple AM-to-AM and AM-to-PM characterization. The complex coefficients polynomial and Saleh model are common examples of these types of models.

- Models with linear memory. These models are necessary when the response of the system is to be analyzed with wide-bandwidth signals. A system with band-pass characteristic will cause a filtering effect that will modify the frequency of the input envelope. Behavioral models can still use AM-to-AM and AM-to-PM characterization but for all the input expected frequencies. A memoryless system cascaded with a low pass filter is the common representation for these models (Weiner and Hammerstein).
- Models with non-linear memory. These models will characterize responses that do not depend exclusively on changes in the input envelope. Some of the physical phenomena that cause these effects were presented on Section 2.2.5. Volterra Series are the most popular method to implement these models, other implementations include the use Artificial Neural Networks (ANN).

### 2.4.2 Power Series

To derive a power series is probably the simplest and fastest way to model a non-linear system. The characteristics of a system like the one represented with equation 2.1 can be analytically derived with the formulations employed on section 2.2. Power series models are usually combined within other models like parametric models where the given parameters can be used to derive the power series or simply to find a relation between different performance characteristics of the device. This is exemplified in section 2.5.2 where a measurement based model (S2D) uses gain compression data to estimate harmonics and intermodulation products. Power series models are limited to memory-less systems with weak non-linear characteristics.

### 2.4.3 Volterra Series

The Volterra Series approach is one of the most often studied methods in non-linear system theory. It presents the advantage over power series methods that it is capable of modeling systems with memory. Volterra Series describe non-linear systems using a multidimensional convolution operation with the general form presented in equation (1.7).

$$w(t) = \int_{-\infty}^{+\infty} h_1(\tau) \cdot s(t-\tau_1) d\tau_1 + \int_{-\infty-\infty}^{+\infty+\infty} h_2(\tau_1,\tau_2) \cdot s(t-\tau_1) \cdot s(t-\tau_2) d\tau_1 d\tau_2 + \int_{-\infty-\infty-\infty}^{+\infty+\infty+\infty} h_3(\tau_1,\tau_2,\tau_3) \cdot s(t-\tau_1) \cdot s(t-\tau_2) \cdot s(t-\tau_3) d\tau_1 d\tau_2 d\tau_3 + \ldots \quad (1.7)$$

The different functions $h_n(\tau_1,\tau_2,\tau_3,\ldots,\tau_n)$ are called n$^{th}$-order kernels and they represent the non-linear impulse response of the system.

Something that can be inferred from equation (1.7) is that it is represented as a series of infinite terms that when converted to discrete time to be handled by a computer will need to be truncated, thus loosing accuracy. Therefore, at some point a compromise between accuracy and complexity will be required; this represents one of the main limitations of the Volterra Series. As the device presents a more non-linear behavior, the total number of kernels needed to keep the truncation error under an acceptable level will increase significantly. In general, Volterra Series analyses are only practical with weakly non-linear devices. Although some efforts have been made in order to simplify their complexity [13] extracting and simulating Volterra Series models can be a tedious process.

## 2.5 Measurement Based Behavioral Models

Measurement based behavioral models differ with the previously described models in that instead of finding a mathematical relation between input and outputs, they map excitation to responses of the system. Once the mapping has been performed the simulator with the help of some indexing will locate the corresponding outputs and introduce them into the flow of the simulation.

The most effective way in which this mapping is achieved is through the use of network parameters. Network parameters provide a relation between input and output currents and voltages, impedance (Z) and admittance (Y) parameters, and between incident and reflected waves, scattering (S) parameters. Impedance and admittance parameters can be easily extracted at lower frequencies; however, they are less meaningful at higher frequencies where the concept of impedance/admittance is arbitrary and the definitions for voltages and currents will be subject to some normalization [14]. It is at higher frequency where the scattering parameters are more effective in characterizing incident and reflected waves.

The network parameters can be accurately obtained with classical network analyzers and can be easily introduced into a computer simulation. However, their validity will be conditioned by the linearity of the circuit they are trying to characterize. Network parameters fail to predict the effects of nonlinear circuit behavior and under these circumstances further analysis is needed in order to obtain an accurate behavioral model.

In this work only S-Parameters are consider since they cover a higher range of applications. Initially, classical definitions for scattering parameters under linear

conditions will be studied and later alternative solutions for non linear systems will be considered.

For a given two port network,

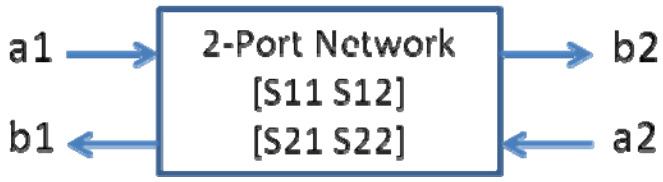


**Figure 2.4 -Two Port Network Representation**

The equations that relate incident and reflected waves are:

$$b_1 = S_{11} \cdot a_1 + S_{12} \cdot a_2$$
$$b_2 = S_{21} \cdot a_1 + S_{22} \cdot a_2 \qquad (1.10)$$

This representation of the S Parameters is widely accepted and is a fast and effective way to characterize a system. The simplest behavioral model that can be generated is a file where S-Parameters versus frequency are presented. These simple models can e easily generated with the use of Vector Network Analyzers (VNA.) S-Parameter models are limited to linear systems and they will fail to predict effects like those presented in section 2.2.When this happens, alternative solutions will be required.

### 2.5.1 P2D

The P2D model is a measurement based behavioral model developed by Agilent and included in Agilent's Advanced Design System (ADS) [2]. This model uses multiple sets of S-Parameters measured under linear (small signal, frequency swept) and non-linear (large signal, power swept) conditions to characterize the device. Each set will be

indexed with one or several variables that will represent the measurement condition (e.g. bias, temperature, substrate.)

In order to characterize the large signal response of the device the model requires multiple power sweeps at different frequencies. If the frequencies required for the simulation are not present in the model interpolated data will be used [4].

The P2D model provides a characterization of amplitude and phase change with increasing power which permits an accurate prediction of gain and phase compression effects and distortion due to envelope-band frequencies [3, 4]. On the other hand, the P2D model is limited to predict distortion only in the fundamental frequency, being incapable of modeling harmonic and intermodulation response.

### 2.5.2 S2D

The S2D model has a very similar structure to P2D where multiple sets of data containing linear and non-linear data are indexed according to variables which represent modeling conditions. The difference between P2D and S2D comes from the way the non-linear data is stored. S2D uses a normalized gain and phase compression characteristic obtained from an S21 power swept measurement. This characteristic will be fitted by the simulator to an odd order polynomial whose coefficients can be used to predict odd order harmonic levels and odd order intermodulation products. This last feature represents an advantage of S2D models over P2D models; on the other hand, S2D models cannot predict changes in the other three S-Parameters versus power.

The S2D model does not interpolate between large signal frequencies; therefore, all the frequencies needed for the simulation must be accordingly characterized in the model.

### 2.5.3 Poly-harmonic Distortion Model (PHD)

The Poly-harmonic Distortion model (PHD) implements a model where a relation between inputs and outputs can be found even when these signals are at different frequencies. In this way, a relation between the input at the fundamental frequency and the different harmonics can be characterized. The PHD model is often considered as an extension of the S-Parameters [5] by way of a more complex data file input.

The PHD model has been named differently among literature. Initially, it was referred to as Large Signal S-Parameters [15] which was also a common way to name power swept S-Parameter data. Later it was more formally defined as Poly-harmonic Distortion (PHD) model [16, 5]. The PHD model is also classified and commonly known as Large-Signal Scattering function. Finally, the first commercial implementation of the model, included in Agilent ADS [2], uses an input file set called X-Parameters.

X-Parameters represent a natural evolution from the S-Parameters and provide a relation in magnitude and phase between inputs and outputs at different frequencies. The model is usually expressed using a scattering function of the following form.

$$B_{mk}^{N} = \sum_{nh} S_{mknh}\left(A_{11}^{N}\right)A_{nh}^{N} + \sum_{nh} S'_{mknh}\left(A_{11}^{N}\right)A_{nh}^{N^{*}} \qquad (1.11)$$

It can be seen how the scattered wave quantities $B_{mk}^{N}$ are represented as a function of the input wave at the fundamental frequency $A_{11}^{N}$. The superscripts N on the wave quantities indicate that the values are normalized in amplitude and phase to the input fundamental frequency. The subscripts *mk* refer to the k$^{th}$ frequency component coming out of port m$^{th}$, and the subscripts *nh* refer to the h$^{th}$ frequency component going into port n$^{th}$.

The scattering function is implemented through the complex values $S_{mknh}$ and $S_{mknh}^{'}$ which represent a linearization of the response of the Device Under Test (DUT.) This linearization was developed by Verspecht et al on [17] and includes the novelty of the conjugate term $S_{mknh}^{'}$. The use of the conjugate term overcomes the limitation of common S-Parameters to represent a device whose phase response decreases as the phase of the excitation increases, as it will occur with the image frequency of a mixer. This methodology was previously developed by Maas [18] and Williams et al [19] for use in mixer characterization and is formally applied to the PHD model by Root et al [16], and Vesperch et al [5].

### 2.5.4 A Simplified PHD Model

One of the drawbacks of the PHD model is the need for advanced measurement instrumentation that allows measuring the amplitude and phase of all the frequency components scattered and incident from/to the DUT. Large Signal Network Analyzers (LSNA) [20] will have the ability to extract all the wave components required to

determine the scattering function; but, at the time of the writing of this document, LSNA are not widely available.

An alternative model, presented by Liu et al in [6], can be extracted with regular VNAs combined with a load-pull system, if the DUT can be assumed unilateral ($S_{12}$=0) and only the fundamental frequency is considered. With the previous assumptions we can represent $B_2$ as:

$$B_2 = S_{21}A_1 + S_{22}B_2\Gamma_L + T_{22}B_2^*\Gamma_L^* \tag{1.12}$$

If we introduce a tuner into the measurement setup that enables measurements of the S-Parameters for different values of $\Gamma_L$, with the appropriate fitting all the coefficients can be computed to build the scattering function.

## 2.6 Conclusions

An overview of behavioral modeling theory in general and measurement based behavioral models in particular has been presented. The consequences of non-linear behavior of electronic components in communication systems justify the need for non-linear characterization. Behavioral models represent a practical way to achieve this characterization.

# CHAPTER 3

# NON-LINEAR MEASUREMENTS WITH VECTOR NETWORK ANALYZERS

This chapter presents some approaches associated with linear and non-linear measurements with Vector Network Analyzers (VNA). It is the purpose of this chapter to provide a review of the measurement procedures and concepts needed for this work. However, other topics associated with non-linear measurements (e.g. load-pull) will not be covered.

## 3.1 Vector Network Analyzer Theory

The introduction of the Vector Network Analyzer (VNA) by Hewlett Packard in the late 60s was a revolution for the RF measurement market. VNAs provided a quick and accurate way to characterize electrical networks by providing a whole set of network parameters (e.g. impedance-Z, admittance-Y, Scattering-S). Features that made the VNA an essential measurement tool in the following years include: the ability to obtain both the magnitude and phase of the network parameters, and the use of vector corrections to de-embed errors due to cables and other imperfections from the measurements.

Figure 3.1 presents the architecture of one of the network analyzers used through this work: the Anritsu 373XXC. The analog subsystem is composed of three main modules: signal source, test set, and receiver [21].

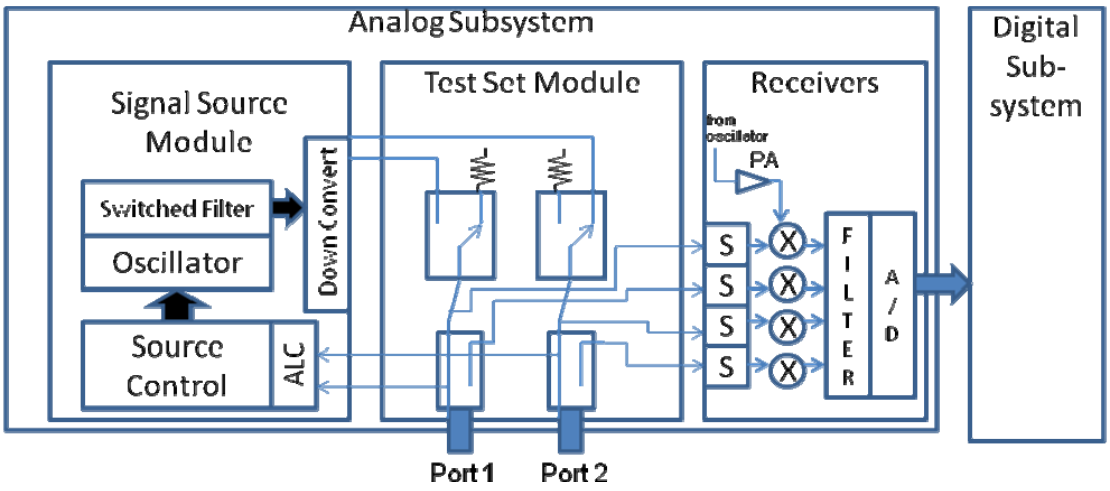


**Figure 3. 1 – VNA Architecture (based on Anritsu 373XXC [21])**

The signal source module will generate the RF signal that will be used as excitation for the device under test. The signal will usually be swept in frequency and the circuitry will receive feedback from the test to ensure appropriate signal leveling and phase lock.

The test set module will route the excitation signal generated by the source module towards the DUT. Both the excitation signal and the response of the DUT will be directed to the samplers of the receiver modules. The test set is mainly composed of the couplers used at the ports to separate incident and reflected signals, the switches that will direct the excitation to the appropriate port or connect to the match, and additional components like step attenuators that will provide flexibility in the setup.

Finally, the receiver module will sample, down-convert, detect, and digitize the signals. Modern VNAs include four samplers that will allow configuring any measurement ratios independently to the source path. This feature enables the VNA to measure the reflection coefficients of the matching loads used in the test set; and, after

correcting for the difference, the 8-term error model calibration algorithms can be performed (e.g. TRL, LRM.)

### 3.2 Vector Calibration

Vector calibration will correct for all the components introduced by the test set and measurement setup to obtain a measurement at reference plane. There are several techniques to achieve calibration with the most commonly implemented methods listed below:

- SOLT. The Short-Open-Load-Thru calibration is based in the measurement of four well known standards whose behavior has been previously characterized [22].
- Complex Short-Open-Load-Thru (cSOLT)[23]. This technique follows the same methodology that SOLT with introduction of more detailed models for load and thru standards. The better characterization of the models improves significantly the results provided by traditional SOLT, typically poor at high frequencies.
- SOLR. The Short-Open-Load-Reciprocal algorithm substitutes the thru standard in a common SOLT calibration by any device whose response is reciprocal ($S_{12}=S_{21}$)[24].
- Complex Short-Open-Load-Reciprocal (cSOLR)[25]. cSOLR combines the use of the same advanced models for the calibration standards used for cSOLT with the capability of using any reciprocal device as the thru standard.
- Through-Reflect-Line (TRL)[26]. This technique relaxes the need of characterization of the standards and can be performed with some reasonable

assumptions about their behavior. Multiline TRL[27], a variation over TRL implemented at NIST, is widely accepted as the most accurate calibration algorithm.

- Line-Reflect-Match (LRM)[28]. LRM requires a standard line (delay or thru) whose behavior is completely known [26], a reflect standard that presents the same characteristic at port 1 and 2, and a match standard (usually assumed perfect) at both ports. The accuracy of LRM depends on the quality of the match standard.

Calibration procedures require measurements of standard DUTs whose behavior is totally or partially known. With uncorrected data of the calibration standards the error introduced by the measurement setup can be characterized. This error is commonly modeled by the 12 error term which uses different flow diagram representations for forward and reverse paths respectively.

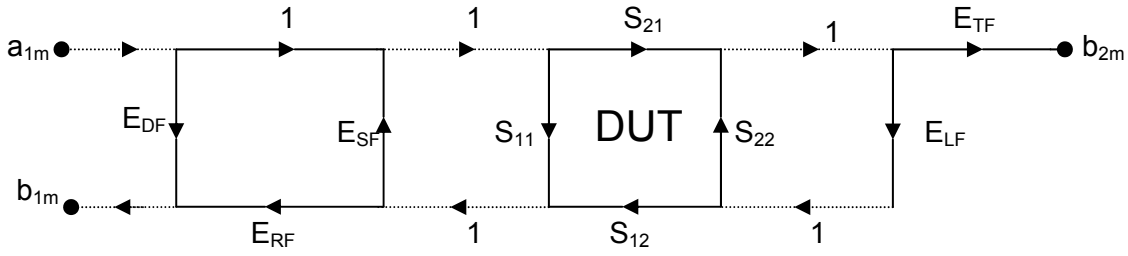


**Figure 3.2 - Error Model (forward path)**

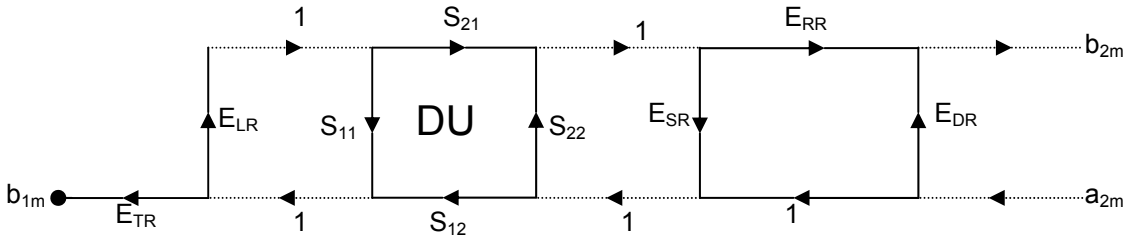


**Figure 3.3 - Error Model (reverse path)**

The meaning of all the elements in figures 3.2 and 3.3 is explained on table 3.1.

**Table 3. 1 – Error Terms**

| Forward Path | Reverse Path |
|---|---|
| $a_{1m}$ = RF leaving port 1. | $a_{2m}$ = RF leaving port 2. |
| $b_{1m}$=RF entering port 1. | $b_{2m}$ = RF entering port 2. |
| $E_{DF}$=Forward directivity. | $E_{DR}$ = Reverse directivity. |
| $E_{SF}$=Forward source match. | $E_{SR}$ = Reverse source match. |
| $E_{RF}$=Forward reflection tracking. | $E_{RR}$ = Reverse reflection tracking. |
| $E_{TF}$=Forward transmission tracking. | $E_{TR}$ = Reverse transmission tracking. |
| $E_{LF}$=Forward load match. | $E_{LR}$ = Reverse load match. |
| $S_{11}$, $S_{21}$, $S_{12}$, $S_{22}$ = S parameters of the DUT. | |

In addition to those presented in figures 3.2 and 3.3, two more error coefficients are needed to complete the model. These two terms are the isolation terms ($E_{XF}$, $E_{XR}$) and they account coupling between port 1 and port 2 of the VNA through any path other than the connection trough the DUT. This effect is usually small and is often neglected. In the two previous flow diagrams, isolation was not included and it will be neglected for the rest of this document.

Another alternative is the 8-term error model [29], which requires correcting for the differences in reflection of the internal termination of the VNAs for forward and reverse paths. This correction needs a 4 sampler VNA that allows the reflection coefficients of the terminations, the so-called "switching terms" to be obtained. The 8-term error model uses one flow diagram to characterize the error of both reverse and forward paths. This feature is the basis for algorithms like TRL or LRM.

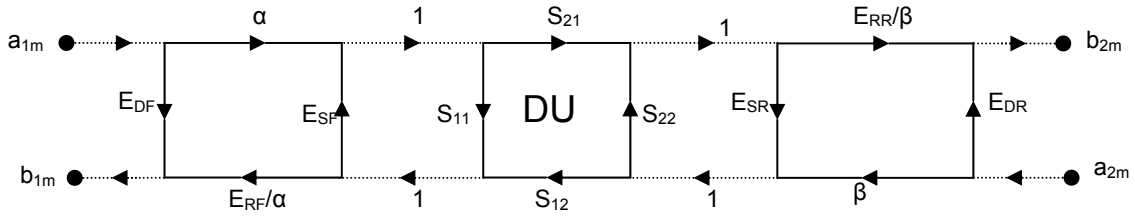


**Figure 3.4 – 8 Term Error Model**

## 3.3 VersiCal

VersiCal™ is a software solution implemented using National Instruments LabVIEW [30] to perform VNA calibrations from a PC. VersiCal obtains data from the VNA and through the use cSOLT based calibration algorithms will compute the error coefficients that will be sent to the VNA. VersiCal uses advanced models for the classical calibration standards (short, open, load, through) to provide accuracy at high frequency comparable to TRL[31]. VersiCal was developed at the University of South Florida (USF) by several research projects directed by Dr. Dunleavy and Dr. Weller. The algorithms implemented as part of this thesis work use cSOLT calibrations and part of VersiCal code.

## 3.4 VNA Non-linear Measurements

Although Vector Network Analyzers are a rapid and accurate way to obtain network parameters, they will be valid only when the DUT is operating under linear conditions. When the device shows non-linear effects the validity of the S-Parameters, and any network parameter in general, is questionable. In spite of this, and depending on the degree of the non-linearity, VNAs can capture some useful information about the response. The following limitations apply to a VNA:

- Conventional network analyzers use their own internal RF Source, which generates a single tone continuous wave. Therefore, multi-tone tests (e.g. intermodulation distortion) cannot usually be performed.
- The purpose of a VNA is to obtain S-Parameters, which are ratios of the input and output voltages incident to and reflected from the DUT. Therefore, absolute power levels cannot be directly measured with VNAs. When this is required, an external power detector will be needed.
- The VNAs receivers are tuned to a predetermined frequency and will capture signals within a limited (IF) bandwidth. The frequency at which the receiver is tuned is usually set equal to the frequency of the RF source. This circumstance impedes VNAs from obtaining harmonics that the DUT may generate. Some VNAs include a frequency offset mode that allows to measure amplitude at frequency other than the generated for the RF; however this mode does not allow obtaining phase, unless a special phase calibrator is available.
- VNAs measure phase by using a phase detector that will produce a voltage signal proportional to the difference in phase between the two signals being ratioed. The basic operation of a phase detector requires phase lock between the two signals and, as a consequence, imposes that both signals need to be at the same frequency. A VNA will therefore be unable to obtain phase information of harmonics or any other frequency component other than the fundamental input.

With the previous considerations this work limits non-linear measurements with VNAs to single frequency AM/AM and AM/PM measurements. In addition, when additional instrumentation can be combined with the VNA additional matching behavior

like HOT S22 response can be extracted. The information provided by these types of tests towards the generation of the models will be explained in the following sections.

### 3.4.1 AM-to-AM

AM-to-AM tests will characterize the change in the amplitude response of the DUT as the power of the input excitation increases. The natural way to measure this effect with a network analyzer is by observing the change in gain ($S_{21}$) as the input power increases. This measurement will require the use of a power meter in order to be able to record the absolute input power that the VNA is driving onto the DUT. VNAs will sweep power at the DUT at a given frequency and measure gain.

These methodologies yield good results if the device is not driven too hard into compression. As the input power increases the harmonic content will become significant enough to change the behavior of the measurement setup (reflections) and could even create problems to the ALC and phase lock systems of the network analyzer.

### 3.4.2 AM-to-PM

In the same manner than AM-to-AM, an AM-to-PM measurement characterizes the change in phase of the response of a DUT as input power increases. The ability of a VNA to measure phase facilitates this test compared to other alternatives available with different instrumentation. The phase of a power swept $S_{21}$ will contain phase compression data. The same restrictions previously mentioned for AM-to-AM apply.

### 3.5 HOT S-Parameters Measurements

In the previous sections, a methodology to obtain non-linear response of a DUT through a continuous wave power swept input excitation was presented. In order to extract AM-to-AM and AM-to-PM behavior only the $S_{21}$ response of the DUT is needed. When the four S-Parameters are to be analyzed versus power, additional considerations are needed. By sweeping power at the input port of the DUT meaningful values for $S_{11}$ and $S_{21}$ can be obtained; however, with a power sweep at the output port of the DUT without excitation at the input the resulting values for $S_{12}$ and $S_{22}$ are questionable. HOT S-Parameter techniques will apply an input signal to the DUT (pump or driving tone) combined with the signal generated by the VNA (probe tone) which will be used to obtain the ratios that constitute the S-Parameters.

#### 3.5.1 Applications of HOT S-Parameter Measurements

Common HOT S-Parameter measurement applications are summarized below.

- Output Matching (Hot $S_{22}$). Hot $S_{22}$ is one of the most popular applications of HOT S-Parameters as it presents a solution to measure the change in the output match of the DUT versus input power. The probe tone coming from the VNA will measure $S_{22}$ for different input power levels of the driving tone. Hot $S_{22}$ measurements are limited to the impedance set by the measurement environment (usually 50 ohms) and will be useful only when the DUT is expected to work under the same reference impedance [32].

- Stability (Hot K-factor). When all the Hot S-Parameters are measured unconditional stability versus input power can be evaluated. Rollet's stability criteria establish that a device will be unconditionally stable if K>1 and |Δ|<1 were:

$$K = \frac{1 - |S_{11}|^2 - |S_{22}|^2 + |\Delta|^2}{2|S_{12}S_{21}|} \qquad \Delta = S_{11} \cdot S_{22} - S_{12} \cdot S_{21}$$

When an amplifier is driven into or close to the compression region, its $S_{12}$ response will increase reducing the K factor and henceforth the stability [32]. Some illustrative results of this effect are presented in [33]. This type of analysis can be further extended with the addition of a tuned load which will permit prediction of oscillation conditions [34].

- Memory effects (Static vs. Dynamic AM-AM and AM-PM). The methodology for gain and phase conversion presented in sections 3.4.1 and 3.4.2 is based on a single frequency power sweep $S_{21}$ measurement. This static measurement does not resemble any of the practical excitations that the DUT will encounter in real life. In particular, long memory effects will not be present in this type of measurements [35]. By using a HOT S-Parameter measurement setup where the driving tone will keep a constant excitation on the DUT, a dynamic AM-to-AM and AM-to-PM measurement can be obtained.

### 3.5.2 HOT S-Parameter Measurement Setups

Probably, the most developed measurement set-up for HOT S-parameter measurements is that presented by Martens and Kapetanic in [36]. Martens performs a previous study of the optimum conditions in terms of frequency and power separation between probe and driving tones. Some of the conclusions are summarized below.

- When the applied driving tone is a continuous wave signal, overlap with the probe tone must be avoided. For this the BW of both tones and the receiver must be considered.
- If the applied driving tone is composed of multiple signals (e.g. a modulated signal) its statistics have to be random enough so it can be ratioed out in the samplers of the VNA.
- The power of the probe tone must be selected so it does not change the response of the device in terms of non-linear response. This means that only the power generated by the driving tone should be accounted for linearity purposes. Martens estimates a value for the probe of 13.3dB below the driving tone.

Additional considerations are made regarding the S-Parameter calibration which can be performed with the probe tone only and should stay constant once the driving tone is applied. The set-up presented by Martens uses IS-95 CDMA signal as the driving tone is combined with the probe tone through the use before accessing to the samplers of the VNA .

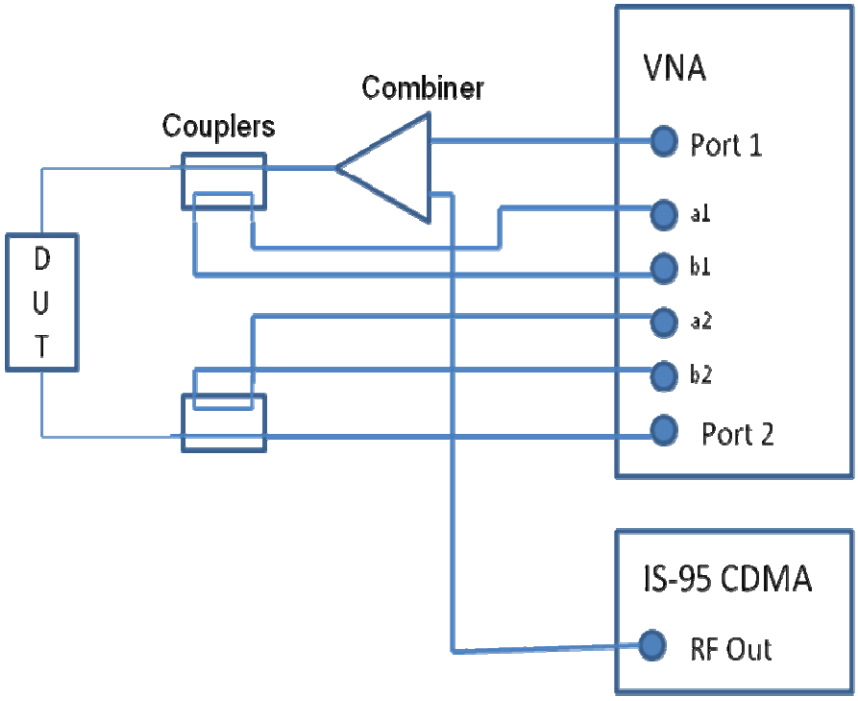


**Figure 3.5 – Martens' HOT S-Parameters Set-up**

### 3.6 Conclusions

Although Vector Network Analyzers were conceived for extracting small signal response, there are some techniques that enable them to characterize non-linear response. These techniques will consist in the measurement of the network parameters at increasing power levels. By observing the change in S-Parameters versus power important non-linear information can be extracted.

# CHAPTER 4

# MEASUREMENT AUTOMATION

This chapter presents an analysis of the methodology developed to automate the measurements proposed on this thesis and to efficiently generate behavioral models. This analysis will include the different capabilities of the available measurement instrumentation and how these can be exploded to improve the time efficiency while maintaining maximum accuracy.

## 4.1 P2D and S2D Models' Syntaxes

As it was mentioned on Chapter 2, P2D and S2D are the measurement based behavioral models selected for implementation. Both models are available in Agilent ADS and are based on text files that contain the data in a given syntaxes. P2D and S2D models will contain multiple segments each of which is uniquely identified by one or several variables. The names and values of the indexing variables can be chosen arbitrarily but they are usually named to represent the measurement conditions under which the data is taken. In this way, if the device is characterized under different bias voltages all the measurements can included into the same model where each measurement/segment is distinguished from the other through the use of a variable (e.g.

bias=8, bias=9, bias=10…) Multiple variables associated to a single segment is allowed too.

Included within each segment are two sub-blocks that will contain linear and non-linear data. For both models the linear data is represented with the classical small-signal S-Parameters versus frequency. The representation of non-linear data is different in both models. This is described below.

### 4.1.1 P2D Model

The P2D model characterizes the four S-Parameters versus power for non-linear data [37]. This is done at several predetermined frequencies. A sample format used for P2D models is presented below.

**Table 4.1 – P2D Model Sample Format**

```
VAR temp=25
VAR Bias=5

BEGIN ACDATA
# AC( Hz S MA R 50)
! small signal s-parameter
% F n11x n11y n21x n21y n12x n12y n22x n22y

!  FREQ       S11M        S11A     S21M       S21A     S12M       S12A     S22M       S22A
500000000          0.9405152 -99.216     0.000955088          154.975    0.000451617          -127.664   0.9435146 -35.187
…
15000000000          0.09941406          12.237     14.18246   35.718     0.002438188          34.376     0.4519666 -
167.315
% F
6000000000
% P1 P2 n11x n11y n21x n21y n12x n12y n22x n22y
-30 -2.614404770 0.057364526 -80.756597974 23.403443437 0.762687047 0.001494666 87.373782083 0.082735885
149.820959273
…
-10 12.829338853 0.010625268 73.381050725 13.850547552 6.528231284 0.001310584 85.236357583 0.082469349
150.093059008

% F
7750000000
% P1 P2 n11x n11y n21x n21y n12x n12y n22x n22y
-30 -2.89084773 0.06095156 174.70866255 22.67031806 -131.446208 10 0.00205907 10.36270271 0.067880976 -122.88631697
…
-10 10.83032021 0.07268953 -178.67085618 11.00312408 -122.05874775 0.00197102 7.64982801 0.06918811 -123.41057121

% F
9500000000
% P1 P2 n11x n11y n21x n21y n12x n12y n22x n22y
-30 -2.61214533 0.03489414 38.49742539 23.40953209 106.23037760 0.00256868 -61.09879751 0.10490100 -161.59140654
…
```

**Table 4.1 (Continued)**

```
-10 12.24506423 0.00883659 107.16773802 12.94950630 118.04732554 0.00276157 -64.32207102 0.104638415 -160.87279921
% F
11250000000
% P1 P2 n11x n11y n21x n21y n12x n12y n22x n22y
-30 -2.76033084 0.03797709 -162.20205672 23.01354158 -19.88360875 0.00359700 -148.97046263 0.11643487 -145.24050048
…
-10 12.80474054 0.03898514 159.81404403 13.81137849 2.19224392 0.00352175 -142.76936481 0.11565502 -146.24074610
% F
13000000000
% P1 P2 n11x n11y n21x n21y n12x n12y n22x n22y
-30 -3.92236293 0.0956123 -3.40350998 20.13176505 -147.83023141 0.00358038 141.20909873 0.19712932 -173.73866194
…
-10 13.55197568 0.09616938 5.50389720 15.05215854 -135.74650659 0.00357466 141.67320887 0.19800575 -173.77536759
END   ACDATA

VAR temp=25
VAR Bias=6
BEGIN ACDATA
# AC( Hz S MA R 50)
! small signal s-parameter
% F n11x n11y n21x n21y n12x n12y n22x n22y
!  FREQ       S11M        S11A      S21M        S21A      S12M        S12A      S22M        S22A
500000000              0.9410584 -99.282     0.00158529             131.243     0.000247891  -107.815  0.9428441  -35.187
…
```

On table 4.1 there are two segments of data identified by the variables for temperature (temp) and bias. Each segment starts with a frequency swept S-Parameter measurement tagged with the string *"% F n11x n11y n21x n21y n12x n12y n22x n22y."* Next, several power swept S-Parameters measurements are included separated by the string "*% F*" followed by the frequency under which the measurement was taken. This model requires specifying the absolute power values being swept at the input and at the output of the device for measuring $S_{11}$ and $S_{22}$, and $S_{12}$ and $S_{22}$ respectively. Input and output power levels are labeled in the headings of every block as $P_1$ and $P_2$.

### 4.1.2 S2D Model

The S2D models follows the same structure than P2D but it limits the non linear data to gain and phase compression. S2D will contain $S_{21}$ normalized values at different frequencies. The normalization will be done at the small signal value of $S_{21}$ that can be

taken from the lowest value of the power swept measurement or from the linear data at the corresponding frequency. A sample format used for S2D models is presented below.

**Table 4.2 – S2D Model Sample Format**

```
VAR temp=25
VAR bias=5
BEGIN ACDATA
# AC( Hz S MA R 50)
! small signal s-parameter
% F n11x n11y n21x n21y n12x n12y n22x n22y
!  FREQ        S11M         S11A       S21M         S21A       S12M         S12A       S22M         S22A
500000000 0.94148 -1.736881858 0.001572796 2.574796979 0.000576968 2.163492687 0.9426413 -0.612366221
…
15000000000 0.1035959 0.77981311 16.46966 0.883014428 0.002813327 1.009934772   0.3627136 -2.302909588
END   ACDATA
BEGIN GCOMP7
#AC ( GHZ S DBM MA R 50 )
% F
6.000000
% P1  n21x n21y
-30.000000000 0.984465340 0.029888495
…
-10.000000000 0.578384979 0.154093235
% F
7.750000
% P1  n21x n21y
-30.000000000 0.985649817 0.005859499
…
-10.000000000 0.497501531 0.156727796
% F
9.500000
% P1  n21x n21y
-30.000000000 0.981097421 -0.003443335
…
-10.000000000 0.568365936 0.193929966
% F
11.250000
% P1  n21x n21y
-30.000000000 0.989023909 0.028655459
…
-10.000000000 0.613054906 0.397279583
% F
13.000000
% P1  n21x n21y
-30.000000000 0.986278367 0.019920132
…
-10.000000000 0.740719172 0.257979192
END         GCOMP7
```

## 4.2 Data Extraction Process

Having reviewed the data required by the models, an analysis of the measurement process is conducted. The general measurement setup used for these models is presented below.

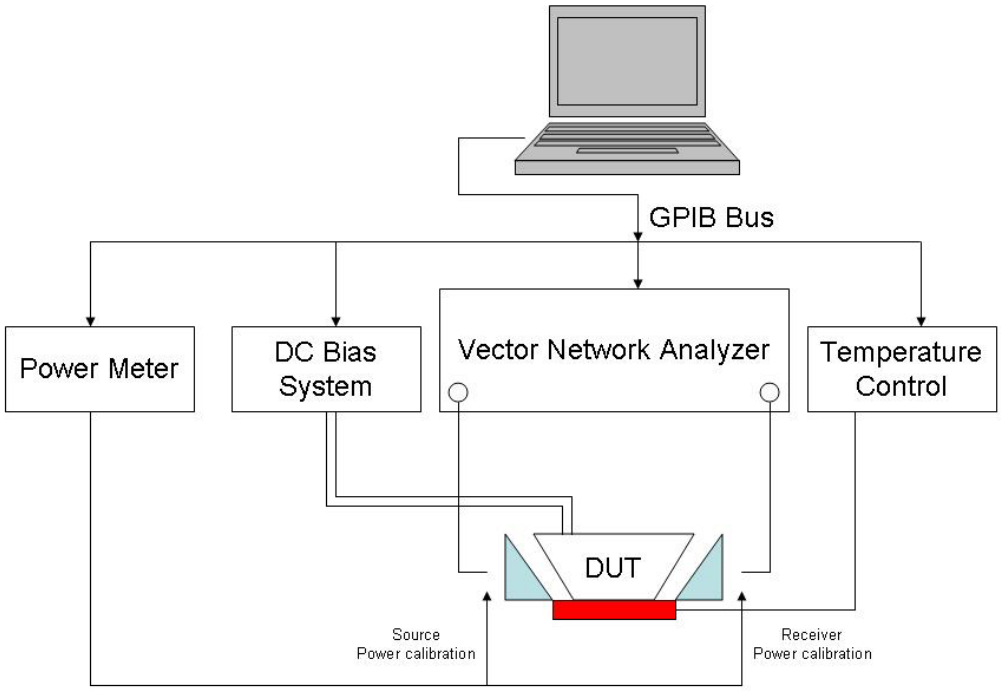


**Figure 4.1 - General Measurement Setup**

As we can see on figure 4.1 the measurement is centered on the VNA that will take the S-Parameter data under both linear and non-linear conditions. The rest of the equipment will be used to set the modeling/measuring conditions; and, in the case of the power meter, to provide the VNA with a reference for absolute power measurements. For the purposes of this thesis we will work with two popular vector network analyzers: the Agilent 87XX Series and the Anritsu Lightning Series. The power meter used is the Anritsu ML2438A.

### 4.2.1 Power Sweep Measurements with Network Analyzers

For generating the model, the network analyzer must measure S-Parameters versus frequency and power. Performing power swept measurements at a continuous frequency is a capability that many network analyzers include; however, some of them will present some particularities regarding on how this is handled. A power swept measurement is performed at a single frequency and changing power. Some VNAs are set up to do this for the four S-Parameters, while others sweep power only for uncorrected magnitude and phase of $S_{21}$ (AM-AM and AM-PM.)

### 4.2.2 Power Calibration

A requirement for generating an accurate model is to know the actual absolute power level going into the DUT. This is a task that the VNA cannot perform on its own since the VNA receivers are not capable of measuring absolute power. In addition, the measurement setup may introduce attenuation/gain that may modify the power that the RF source of the VNA is giving out. The use of a power meter will provide for a reference for absolute power to the VNA with two possible solutions on how use this reference. The usual way to use the power meter is to measure each power setting set during the sweep and readjust the RF source of the VNA until the power meter reads the desired level. This procedure is commonly implemented by network analyzer firmwares and used not only for power swept measurements but also to perform calibration for flatness with frequency sweep measurements. This method may be difficult to implement when the measurement setup introduces significant losses/gain making it difficult for the RF source for the VNA to reach the desired power level. A second alternative is to

estimate the power at the reference plane while building the measurement setup and then record all the powers values with the power meter. The obtained values will be used in the model/measurement as a post measurement x-axis correction to powers set and recorded by VNA during the measurement.

### 4.2.3 Vector Calibrations

In this work, non-linear response is measured through the four S-Parameters (for 2 port DUTs) versus power. Therefore, vector correction will be required so the measurements are obtained at the desired reference plane. Different settings will be required in the VNA for different configurations (frequency sweep and power sweeps at different frequencies.) Measurements of the calibrations standards will be required for each of the different configurations making the calibration process the stage that will consume more time during the generation of the model. This situation and its possible solutions will be studied in Section 4.3.

### 4.2.4 Measurement Conditions

As the purpose of this work is to generate a measurement based behavioral model that will represent the device under different working conditions, we will have to measure it under all these conditions. This will usually include one or several bias voltages, temperatures, and substrates. Linear and non-linear S-parameter data will be taken for each of the possible combinations making the process tedious and time consuming. The accuracy of the model will depend on a high degree on the total number of points measured as these types of models relies on interpolation in order to simulate those

conditions that were not actually measured. Therefore, a balance between the number of modeling conditions and total measurement time should be previously studied. All these issues and their solutions will be addressed in following sections of this chapter.

### 4.3 Quantifying the Measurements

In order to quantify the measurement, a fictitious amplifier to be modeled under certain conditions is presented on table 4.3.

**Table 4.3 - Fictitious Amplifier Used to Quantify the Measurements**

| SAMPLE AMPLIFER | |
|---|---|
| Modeling Condition | Values |
| Voltage 1 (Bias) | 12V., 15V., 16V. |
| Voltage 2 (Control) | -5V., -4.7V., -4.3V., -4V., -3.8V. |
| Temperature | -10C., 25C., 60C. |
| Substrates | PCB1, PCB 2 |
| Frequencies for power sweep | 300Mhz, 600MHz, 1GHz, 2GHz, 3GHz, 4GHz, 6GHz, 8GHz |
| Samples to characterize | 3 samples |

A first initial approach, where all the measurements and calibrations are performed manually is summarized on table 4.4.

**Table 4.4 – Quantification and Time Estimation for the Proposed Amplifier**

| Meas. Type | Quantification | Estimated Time |
|---|---|---|
| VNA DUT Measurements | 3(Bias)x5(Control)x3(Temp)x2(Substrate) x3(samples)x(1(freq.S)+8(pow.S)) =2,430 Swept Meas. | ~ 85 hours 2 min. avg. per measurement (incl. manual adjustments and 1 min per connection) |
| | 162 Connections / Probings | |
| | 405 Manual adjustments of Bias, temperature, and VNA configuration. | |
| SOLT Calibrations | 4(SOLT)x(2(PCB1, PCB2)x(1(freq.S)+8(Pow.S.)))= 72 Connections / 72 Swept Meas. | 18 calibrations taking: ~ 6 hours |
| Power meter measurements | 8(Pow.S.) requires 8 absolute input power measurements or calibrations | ~ 0.5 hours |

As presented on table 4.4 the total time employed in the measurements for this sample amplifier could reach 100 hours. Therefore, it is justified to find an approach to simplify these procedures.

## 4.4 Automating VNA Configurations

The process that consumes more time and can be the source of potential errors in the sequencing of the measurement is setting the different configurations in the VNA. If done manually, a new DUT connection/probe is required every time that we change from frequency sweep to power sweep and even from different frequencies when performing

power sweeps. In addition, for every configuration in the VNA an S-Parameter calibration is required.

A first approach for the automation of the process will consist in the automation of the configurations from a local computer that communicates with the network analyzer through the GPIB. This automation will sequence the configurations automatically so the total number of connections/probes is minimized. The flow diagram for this algorithm is presented on figure 4-2.

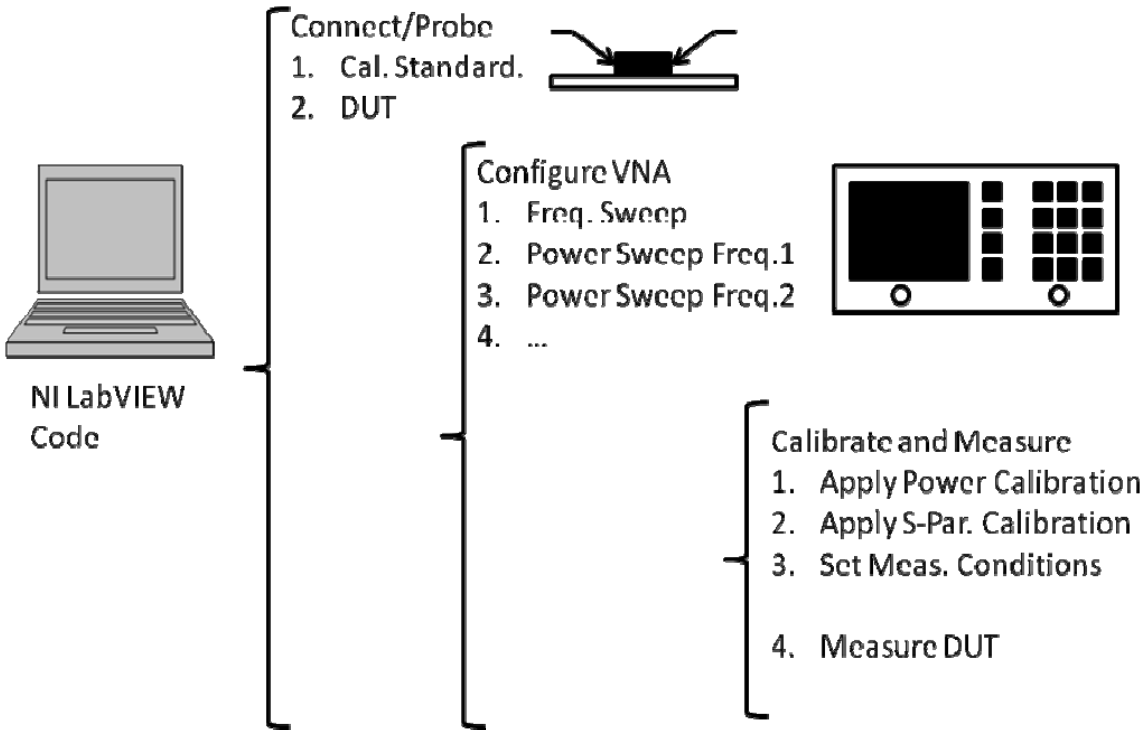


**Figure 4.2 - Sequence for Automatically Setting the Configurations.**

Figure 4.2 is further explained with the following list.

- Step 1: Connect calibration standard.
- Step 2: Set configuration on the VNA.
- Step 3: Measure Calibration Standard.
- Step 4: Repeat steps 2 to 3 until all the configurations are measured.

- Step 5: Repeat steps 1 to 4 until all the calibration standards are measured.
- Step 6: Compute error terms.
- Step 7: Connect DUT.
- Step 8: Set configuration on the VNA.
- Step 9: Apply error terms to VNA.
- Step 10: Set Measurement conditions (bias, temperature, etc..)
- Step 11: Measure DUT.
- Step 12: Repeat 10 until all measurement conditions are measured.
- Step 13: Repeat steps 8 to 12 until all configurations are measured.
- Step 14: Repeat steps 7 to 13 until all DUTs (samples, substrates, etc…) are measured.

The main achievement of this procedure is the reduction of the number of connections of calibration standards and DUT required. All the steps previously listed are sequenced by using LabVIEW code that communicates with the instrumentation through the GPIB. The error terms needed for calibration will be performed locally in the computer using the cSOLT algorithm [23].

### 4.5 Efficient Calibration Algorithm

Additional considerations in terms of time efficiency can be made with respect to the calibration procedures. Following the automation presented in the previous section and in order to perform the calibrations, the standards will be measured under all the configurations required for the VNA. That is, the open, short, load, and through standards

(for SOLT and cSOLT calibrations) will be measured once for frequency sweep, and once for every of the frequencies under which we are performing power sweeps. This procedure can be improved if the error terms computed for a certain configuration can be reused for the other configurations. In this section the conditions under which this assumption can be made are established.

### 4.5.1 VNA Receiver Compression

The receivers of a network analyzer filter, down-convert, and detect the signals to be measured. The response of the receivers will present power dependence (i.e. non-linear) after a certain level. This situation can be a concern especially when measuring amplifiers whose output may drive enough power into the VNA so their response may disturb the measurement. A comprehensive study of the effects of receiver compression based on the change on the error terms obtained with S-parameter calibrations is presented in [38]. As the generation of the models presented in this work may require handling relatively high power levels receiver compression will be an important factor to consider in all measurement setups developed in this work. In general, receiver compression will be avoided by adding sufficient attenuation between the output of the DUT and the ports of the VNA.

Keeping the power at levels below the receiver compression point is one of the conditions imposed to assume that calibrations performed with different configurations of the VNA will stay constant.

### 4.5.2 VNA Internal Attenuation

The test set of a network analyzer will route the excitation generated by its RF source to the DUT and will take its response to the samplers. When the calibration is performed, the response of all the elements in the path between the samplers and the DUT are accounted for. After that, any change in the test set will introduce an error in the calibration.

An analysis of commercial VNAs shows that the most common case of change in the test set occurs in the internal attenuation used either for protection from high input power levels or for modifying the power level of the excitation signal generated by the VNA.

In order to analyze how much a change in the internal attenuation of the VNA affects the calibration, several tests were performed with the Agilent HP8753D. This VNA will change attenuation settings when in power sweep mode to achieve the desired power values. Given five calibrations were performed with the following power ranges:

- Calibration 1: RF level=-20dBm;  power sweep from -25 to -5dBm.
- Calibration 2: RF level=-20dBm;  power sweep from -20 to 0dBm.
- Calibration 3: RF level=-15dBm;  power sweep from -15 to 5dBm.
- Calibration 4: RF level=-5dBm;  power sweep from -15 to 5dBm.
- Calibration 5: RF level=0dBm;  power sweep from -15 to 5dBm.

Within the previous five calibrations, the three firsts imply three different attenuation settings as they use three different power ranges. On the other hand, the last three, although performed at different power levels, will not require change in the internal

attenuation of the VNA. Two of the error term values for each of the calibrations are plotted in Figure 4.2.

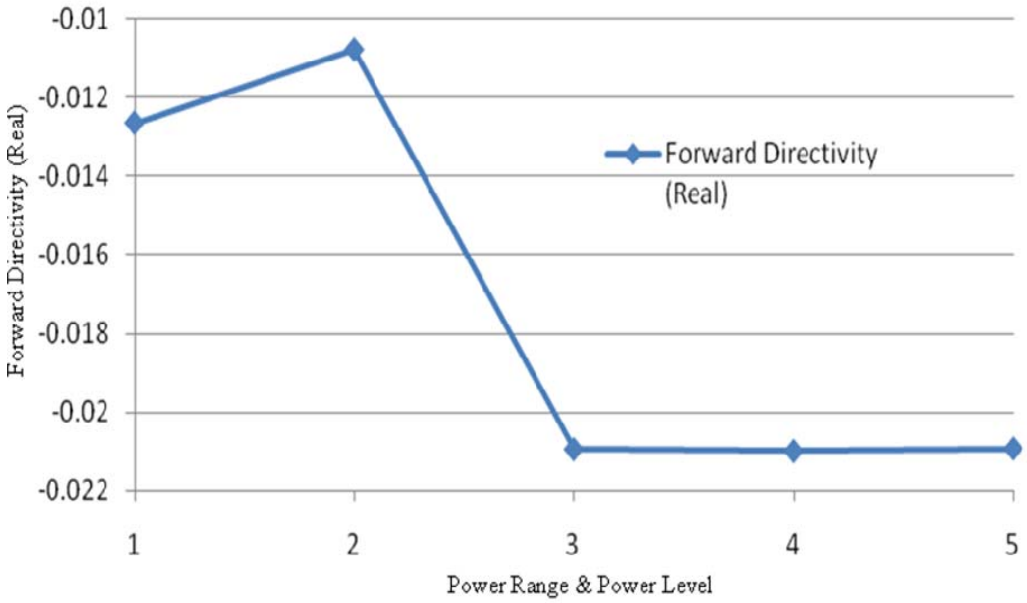


**Figure 4.3 - Forward Directivity (real part) Versus Internal Attenuation.**

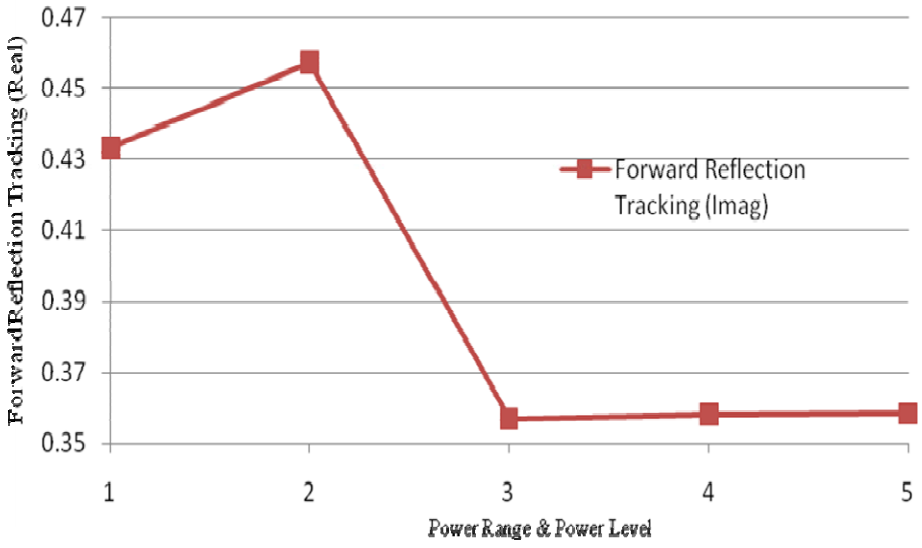


**Figure 4.4 – Forward Reflection Tracking (Imaginary part) Versus Internal Attenuation.**

On figures 4.3 and 4.4, it can be seen that in the first three points there is a change in the error term value as they represent three different power sweep ranges with three

different attenuation settings in the VNA. On the other hand, the three last points in the plots which represent three different RF power levels but within the same power sweep range do not show any significant change. Another test performed was an error bound calibration comparison using the techniques developed by Marks et al in [39]. This test provides the maximum error in an S-parameter measurement performed with two different calibrations.

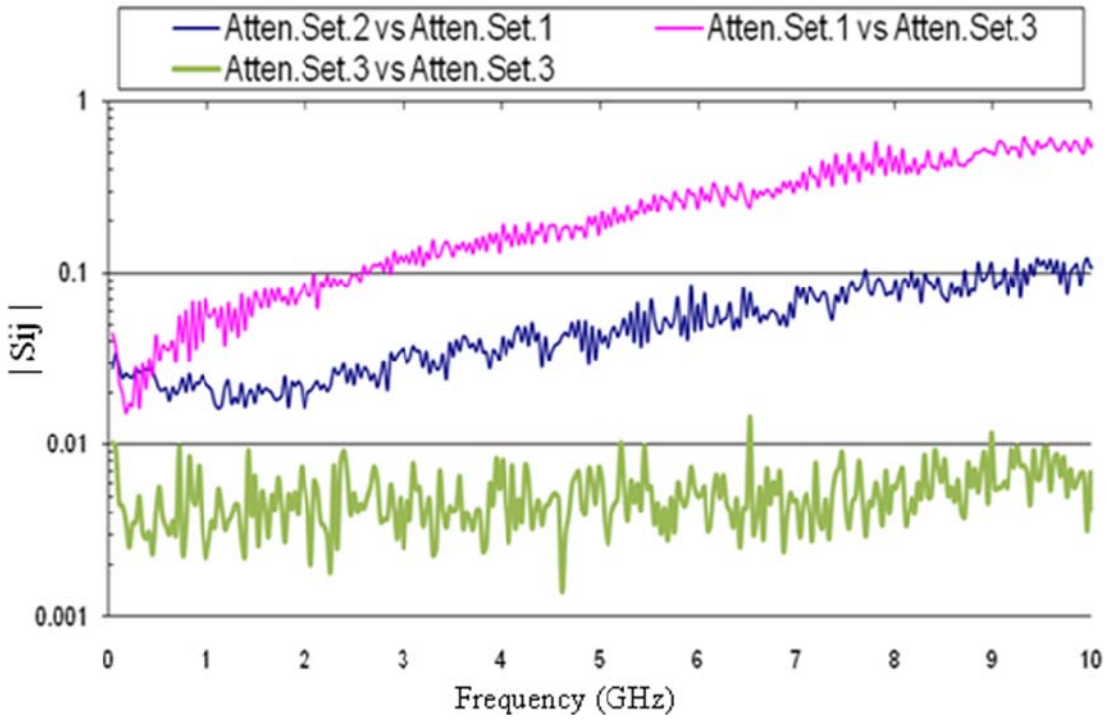


**Figure 4.5 - Error Bound Comparison between Four Sets of Error Terms.**

On figure 4.5, the labels attenuation settings 1, 2, and 3 correspond to the three configurations listed previously. The plot can be interpreted as the error that will result if error terms are assumed constant with change in the settings of the VNA. The line that presents the lowest error corresponds to error terms with same power ranges. This error is negligible and is below the typical level of a repeatability test. The other comparisons show more significant error.

### 4.5.3 Algorithm for Efficient Calibration

Given the previous analysis, it can be concluded that the error terms can be assumed constant if the following conditions are met:

- The power coming into the ports of the VNA stays under the (e.g. <0.1dB) power compression point of the samplers of the VNA.
- The internal attenuation of the VNA remains constant.

With the previous conditions and assuming that all the elements in the measurement setup present linear behaviors with respect to power, a methodology to reduce the calibrations used to obtain the measurements will be developed. Based on a previous analysis of the settings applied by the VNA, the minimum number of calibrations needed can be inferred.

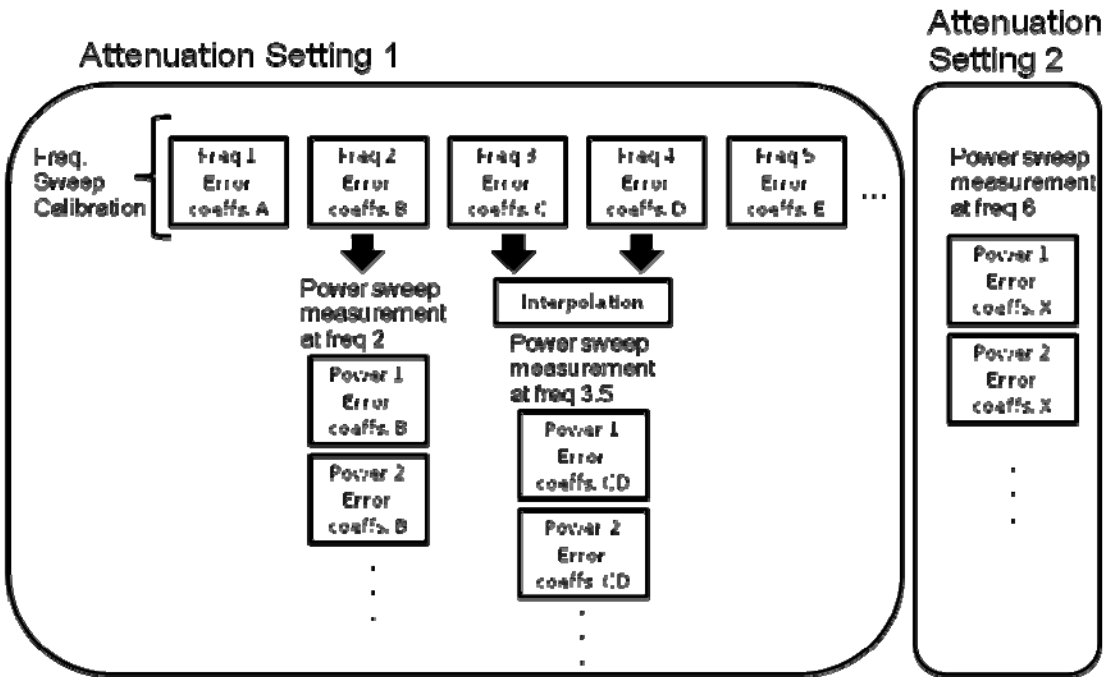


**Figure 4.6 – Algorithm for Efficient Calibration.**

In figure 4.6, it is illustrated how by identifying the configurations needed in the VNA, the error terms obtained for the frequency sweep calibration can be reused and applied to the power sweep measurements.

## 4.6 Application for Calibration Automation

The previous analysis presented on automation of VNA configurations and efficient use of the error terms, are implemented through several LabVIEW applications that will put into practice these algorithms. These applications are a first stage in the generation of the model where power and S-parameter calibrations are performed and stored as a set of files that will be used later by the measurement application. The applications were developed to support the Agilent HP87XX Series and the Anritsu Lightning Series. Both VNAs have different capabilities and although the methodology is the same they both will require specific solutions. In all the cases, the code will communicate with the instrumentation through the classical GPIB bus.

### 4.6.1 Agilent HP87XX Series

The Agilent HP87XX Series capabilities include calibrated power sweep measurements of the four S-Parameters, and power source calibration with a power meter. This is basically all the functionality needed for the data extraction of the data required by the model. The code will simply sequence the required instructions to automate the process through the GPIB bus.

The user's interface of the application that automates the calibrations with the HP87XX is presented on figure 4.7.

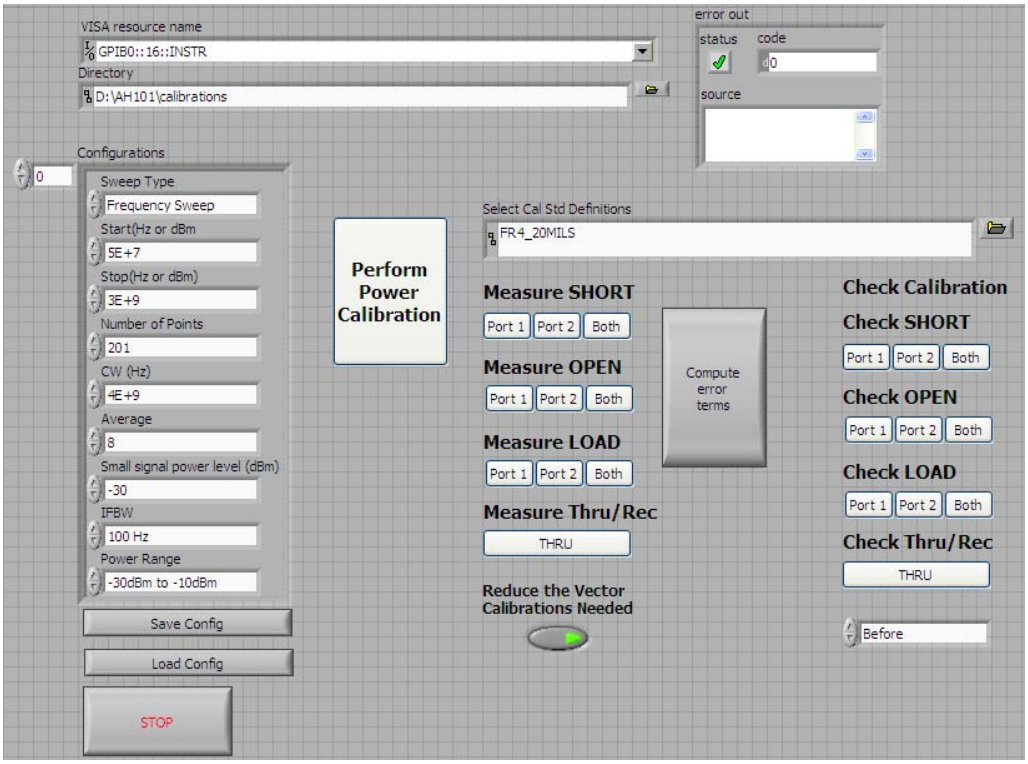


**Figure 4.7 - User's Interface for the Agilent HP87XX Calibration Application.**

The flow of the program is detailed on figure 4.8.

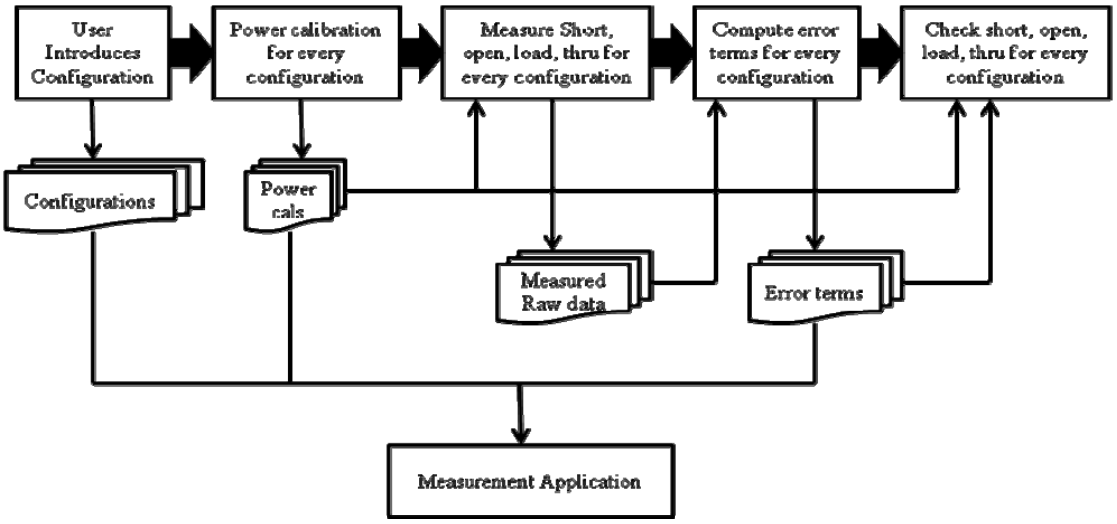


**Figure 4.8 - Flow Diagram for the Calibration Application.**

As illustrated on figure 4.8, the user will initially introduce a list of configurations that will consist of frequencies and power ranges plus other measurement settings like averaging and IF bandwidth. The application will perform each of the following for every of the configurations.

- Power calibration will be performed with the power meter connected to the reference plane, or as close as possible for on-wafer measurements. The VNA will adjust the RF power level of the RF source so the desired power level is measured in the power meter. This procedure will account for any losses in the measurement setup. The program will extract a series of coefficients that will describe the change in the RF source apply them to successive measurements. This is done for every point of all the power sweeps set previously in the configuration.
- The measurements for calibration will obtain raw data from the calibrations standards. The application will decide based on the inputted configurations the minimum number of measurements to take based on the reasoning presented on Section 4.5. The user should probe and connect each of the calibration standards and hit the corresponding button in the users interface. The code will assume that the power calibration has already been performed and will obtain the coefficients form the storage folder. A loop will set each of the configurations in the VNA and take raw data.
- Once all the calibration standards have been measured the user will hit the button labeled as “Compute error terms.” This will generate multiple files with the error terms that will be used to calibrate through the measurements at the different

configurations. These error terms will be later used by the application that will perform the measurements of the DUT.

- Finally, as it is customary to perform a calibration check, the application allows measuring any of the standards with the obtained calibrations. The measurements will be stored in text files using the classical format S2P.

### 4.6.2 Anritsu 37XXX Lightning Series

The Anritsu Lightning Series VNA uses an internal built-in application to perform non-linear measurements. This application will measure gain and phase compression based on uncalibrated measurements so it will not be useful to obtain the four S-parameters as required for P2D. The implemented alternative to directly obtain the power swept S-parameters will perform multiple frequency sweeps at different RF power levels. Once all the measurements have been taken the code will reorganize the data into the format required by the model generation application.

Given the previous characteristics of the Anritsu Lightning, some modifications were implemented to the calibration application used for the Agilent VNA. Figure 4.9 presents the user's interface for the new application.

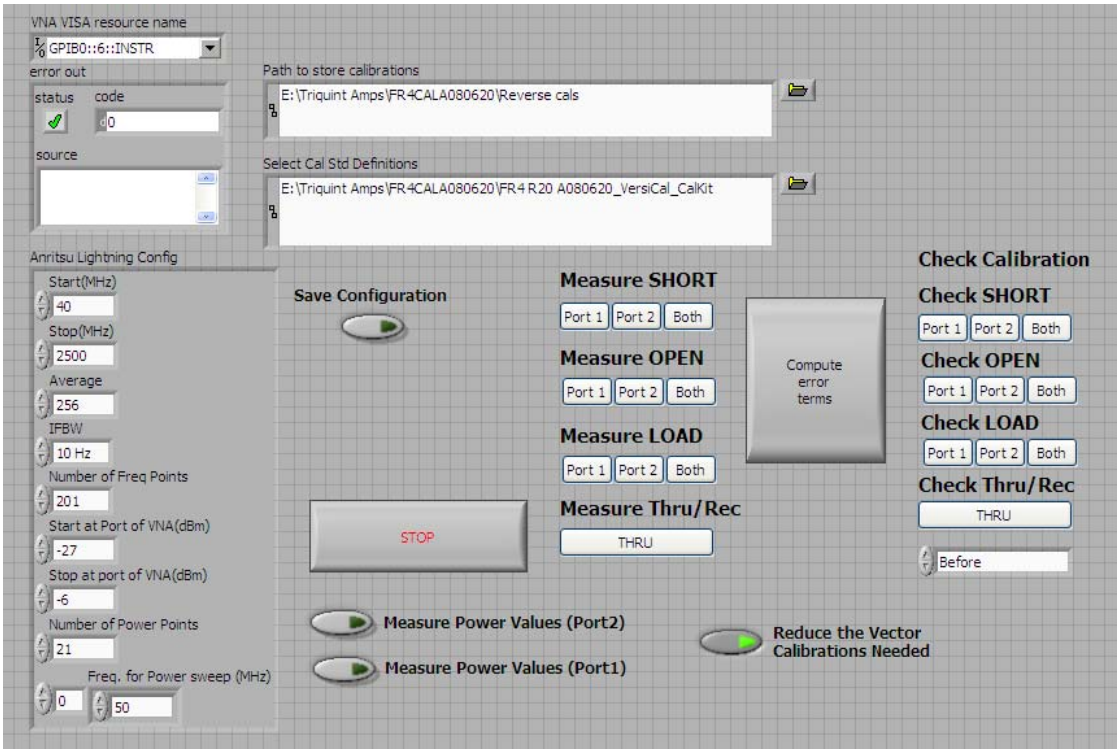


**Figure 4.9 - User's Interface for the Anritsu 37XXX Lightning Calibration Application.**

On figure 4.8, the main functionality of the new application is the same as that described for the Agilent VNA. The only differences are the way the configurations are set in the VNA, and the way the reference for absolute power is implemented.

In the first case, a procedure was implemented to convert from a power sweep to multiple frequency sweeps. This procedure is illustrated in figure 4.9.

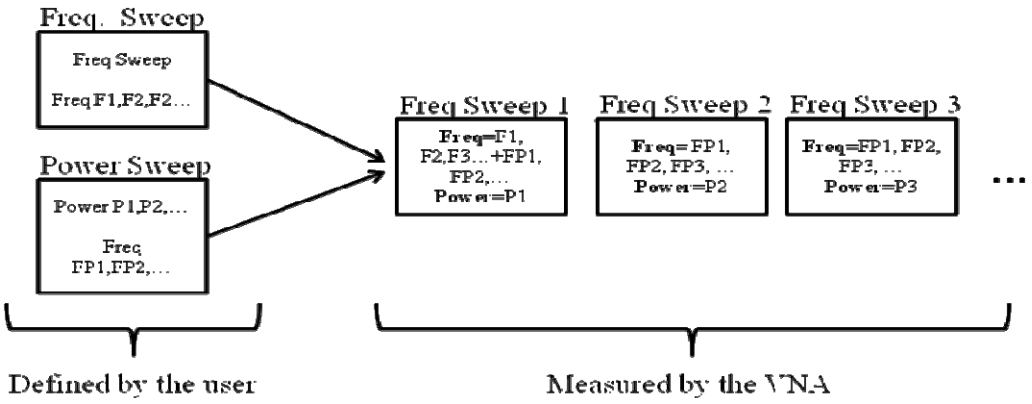


**Figure 4.10 - Conversion from Power Sweep to Multiple Power Frequency Sweeps.**

As presented in figure 4.10, the application will translate a power sweep at multiple frequencies to multiple power sweeps at different power levels. The first frequency sweep will be always the one corresponding to the small signal (linear) data and it will contain a frequency list with the frequencies required for the frequency and power sweeps. The first frequency sweep will also be performed at the first power level of the power sweep. The rest of the frequency sweeps will be performed for the rest of the power points required and only at the frequencies needed for the power sweeps.

The second difference with respect to the application for the Agilent 87XX is due to some problems found when performing calibration for absolute power with the Lightning. With the available VNA, several difficulties were found in achieving power source calibration when the measurement setup introduced some loss. The VNA will not be able to modify the RF level of its source beyond a certain point, and it will fail to set the input power to the DUT to the desired level. The solution presented to this problem is to estimate the power levels to set at the VNA and later measure all the points with the power meter. Thus, the code will set point by point all the combinations between power and frequency in the VNA and measure them with the power meter. All the points will be

saved in a data file that will later be used by the model generation application as the power levels at which the S-parameters were measured.

### 4.7 Application for Measurement Automation

The next step, once all the calibrations have been performed and stored, is to obtain DUT measurements. The DUT measurements will be automated with another LabVIEW application that loops through each of the configurations needed in the VNA, apply the previously computed power (Agilent HP87XX) and S-parameter calibration, and measure under different bias conditions. The user's interface of this application is presented on figure 4.11.

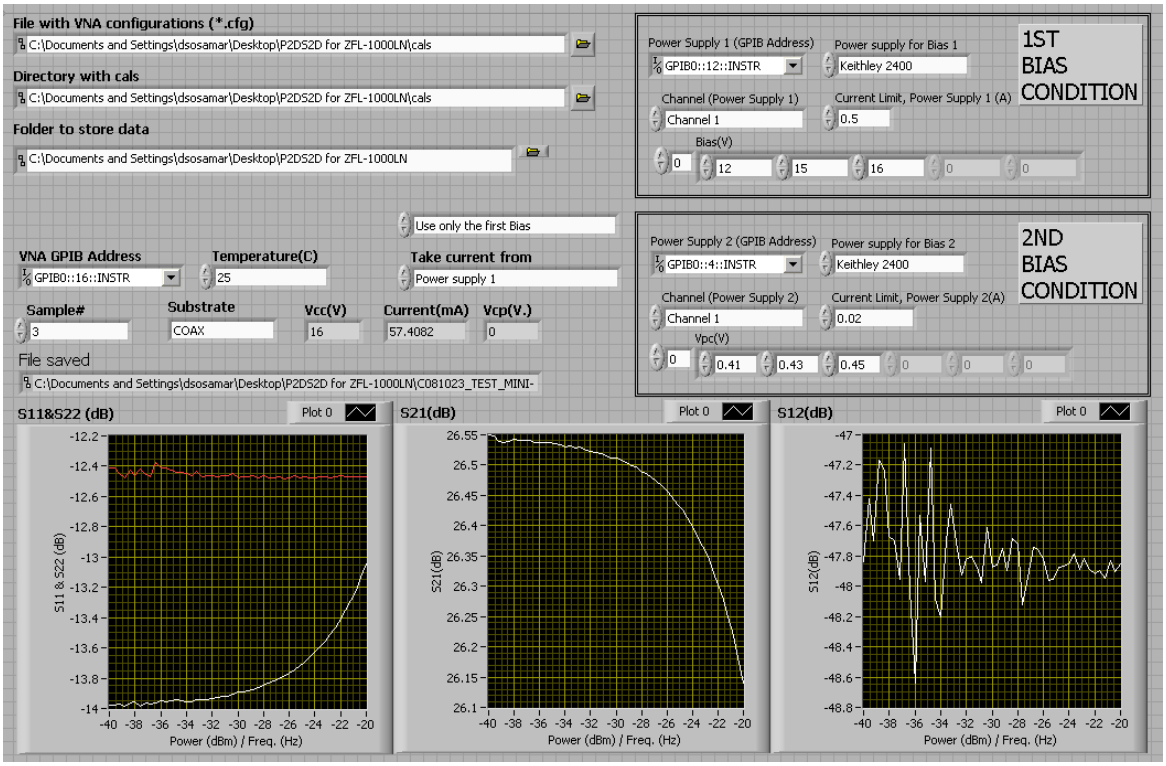


**Figure 4.11 - User's Interface for Measurement Application.**

As shown on Figure 4.11, the application can control to DC power supplies that will set up to two bias conditions. All the possible combinations of bias and VNA configurations will be measured every time the application is run. Other measurement conditions, like temperature, need to be set up manually and the application is run separately for each condition. The application will store all the measured data in text files with filenames that follow a given convention to identify the conditions under which the data was obtained. Later the application for model generation will put the data into the syntaxes of the models.

### 4.8 Application for Model Generation

The application for model generation represents the last step in the whole process of generating the model and will put all the previously taken measurements into the appropriate syntaxes. The user's interface of the generated application is presented on Figure 4.12.

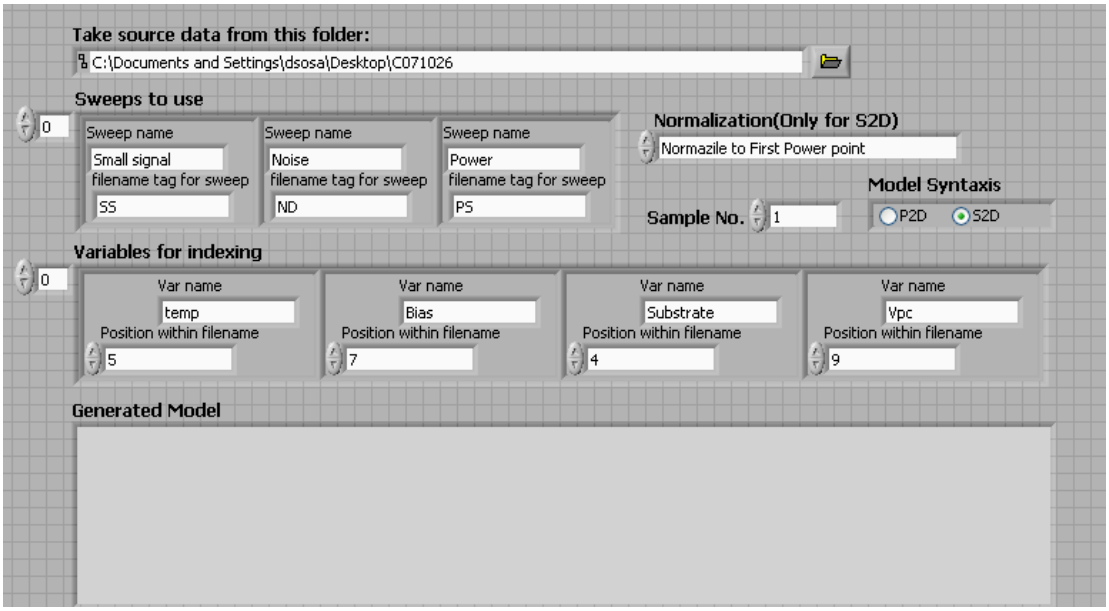


**Figure 4.12 - User's Interface for the Model Generation Application**

The application allows generating the P2D and S2D models that were chosen as examples for this work. This application will require an intermediate stage when using the Anritsu Lightning to convert multiple frequency sweep files each at a different power level to multiple power sweep files each at a different frequency. This stage was implemented as an additional program that needs to be run before the application that generates the model.

### 4.9 Conclusion

This Chapter described the studies performed and the subsequent implemented code to automate all the measurements proposed in this Thesis. A study of the requirements of the models and how they can be efficiently generated with commercial RF measurement instrumentation was conducted. NI LabVIEW code was implemented to automate all the proposed procedures and a significant improvement in time efficiency was achieved.

# CHAPTER 5

# SAMPLE MEASUREMENTS AND MODEL DEMONSTRATION

This chapter demonstrates the use of the procedures and code implemented in this thesis. A commercial surface mount amplifier is measured under different conditions and P2D and S2D models are be generated and simulated.

## 5.1 Measurement Setup

The device to be modeled is the TriQuint AH101 amplifier. This amplifier is mounted on an FR4 20 mils microstrip board and its typical characteristics are listed on Table 5.1 [40].

**Table 5.1 - TriQuint AH101**

| TriQuint AH101 | |
|---|---|
| Frequency range | 50 – 1500 MHz |
| Gain | 13.5 dB |
| Output P1dB | 26.5dBm |
| Supply Voltage | 9 V. |

Based in the previous characteristics a test plan for the measurements can be developed. The selected testing conditions are those presented on Table 5.2.

**Table 5.2 – Selected Testing Conditions for the TriQuint AH101**

| | Small Signal | Large signal |
|---|---|---|
| Frequencies | 40-2500MHz | 50MHz, 100MHz, 200MHz,…,2000MHz |
| Power | -2dBm | -2dBm to +18dBm (21 points) |
| Voltages | 8,9,10 Volts | |
| Temperature | 25 C | |

This test plan will be based on the Anritsu Lightning and will require external amplification in order to be able to drive the device into compression. The Mini-Circuits ZFL-2500VH was used for this. This amplifier has 25dB of gain on the frequency range of 10-2500MHz. The measurement setup used is presented on Figure 5.1.

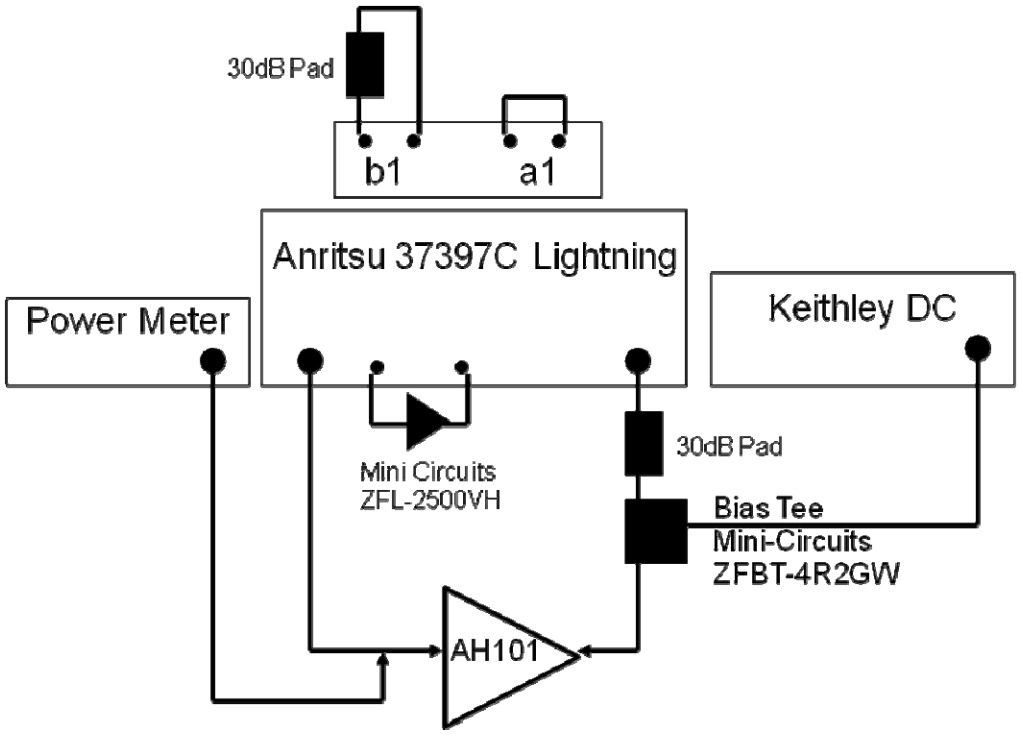


**Figure 5.1 - Measurement Setup**

The first condition established in Chapter 2 needed to perform a minimum number of calibrations while using attenuation to avoid power compression on the samplers of the VNA. According to the Anritsu Lightning documentation [21] this will occur when the power at the samplers is above -10dBm. On Figure 5.1, a 30dB attenuator is included in the external loop connection that access to the 'b1' sampler to reduce the power generated by the amplifier. This power will have a maximum of 18dBm that with an attenuation of 30dB will ensure to be below -10dBm. An external 30dB attenuator is connected to port 2 of the VNA. In this case, losses of the internal couplers before the signal reaches the samplers (7dB) will be accounted for. Therefore, considering that the power swept at the input of the DUT will have a maximum of 18dBm and the compression point of the amplifier is 26.5dBm (output) the output of the amplifier will always be below of 27dBm. With the protection of the 30dB attenuator and the loss of 7dB in the couplers sampler compression is avoided.

The second condition imposed is that the internal attenuation settings of the VNA do not change for the different configuration settings set in the VNA. In order to reach the power levels indicated in Table 5.2, the VNA needs to sweep power from -27dBm to -6dBm. This range of power does not imply change in the internal attenuation of the VNA.

Finally, an extra consideration must be taken into account. In order, for the calibration to remain constant with power all the elements in the measurement setup must show linear response. As the setup requires a pre-amplifier connected to the VNA we have to keep the operation of the amplifier within its linear region. The ZFL-2500VH has

a 1dB compression point at an output of 23dBm. Since the output of the amplifier will be sweeping from -2dBm to 18dBm, we can assume that the measurement setup is linear.

The amplifier is mounted on a 20 mils FR4 board and calibration standards for the same type of board were used. The calibration algorithm used was cSOLT [23] and a previous TRL calibration was perform to extract the models of the standards required by this calibration.

### 5.2 Generated Models

Based on the analysis of the previous section, the required parameters in the applications will be set. Next, the steps detailed on chapter 4 for the generation of the models will be reproduced for this case. An additional step was required. The measurements setup presented in Figure 5.1 introduced some attenuation that was convenient for forward measurements ($S_{11}$ and $S_{22}$). However, this setup will not be able to sweep power for the reverse path since the VNA used for this example does not have an external RF loop for the reverse path. The only possible solution was to flip the device around and perform the measurements twice. Later, with additional code the data will be combined to obtain a single set of data.

Apart from the S-Parameter measurements, absolute power measurements were performed with the Anritsu ML2438A, and all the combinations of S-parameter versus frequency and power were measured and applied to the models.

The models generated were simulated in ADS. A typical circuit schematic for the simulation of a P2D model is presented on figure 5.2.

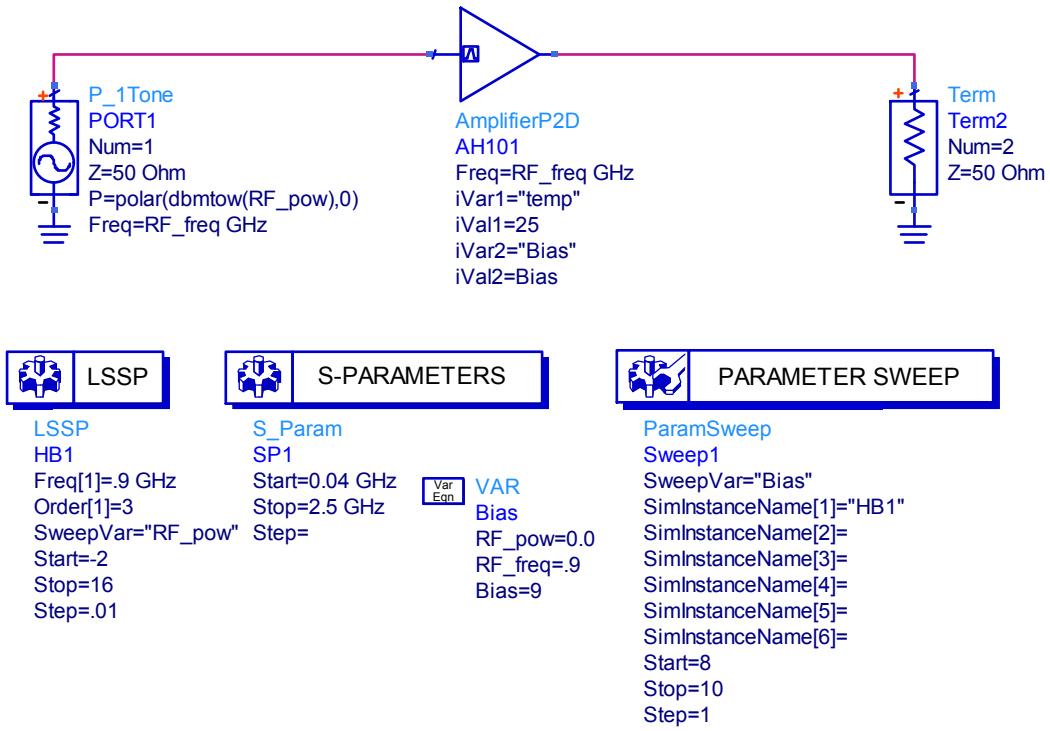


**Figure 5.2 – Circuit Schematic for the Simulation of a P2D Model**

For the P2D model, the response of the device versus power is presented in Figures 5.3, 5.4, 5.5 and 5.6.

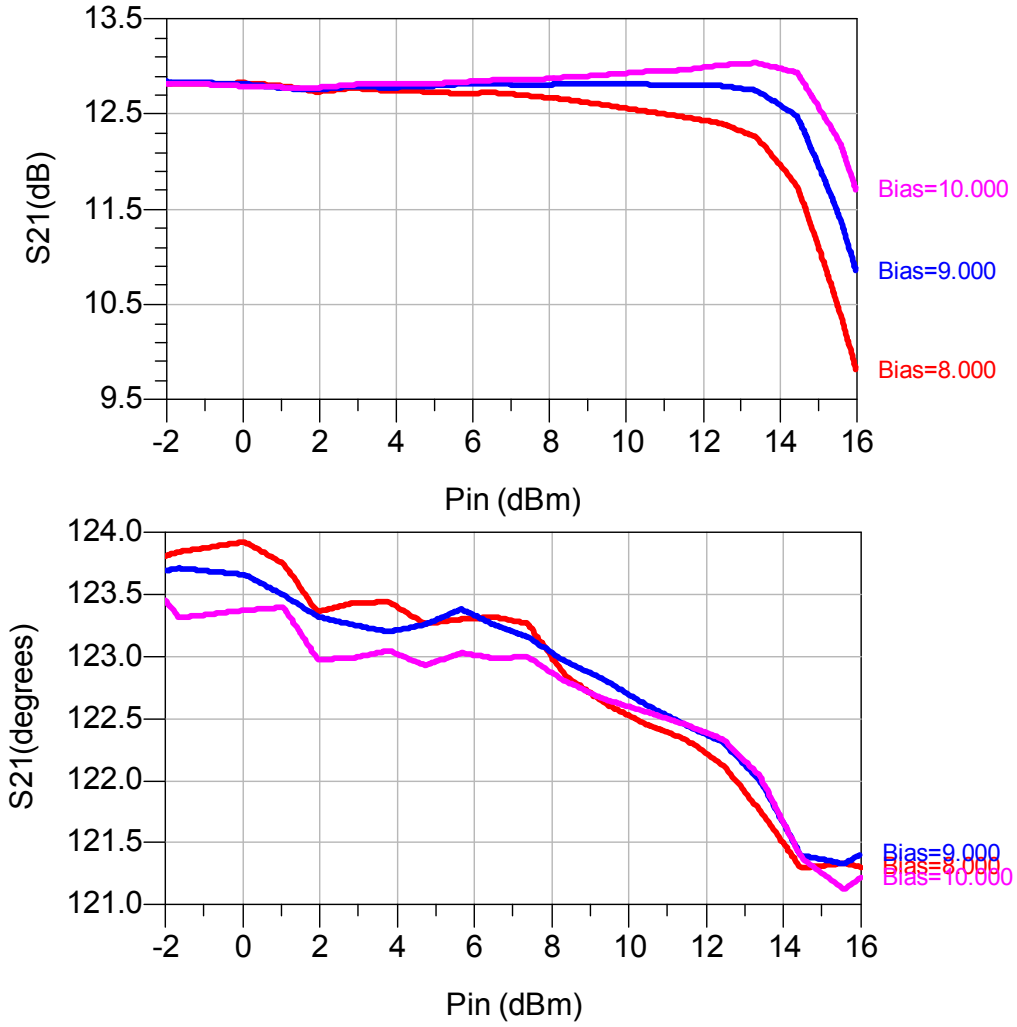


**Figure 5.3 – Gain and Phase Compression of the AH101 Amplifier at 900MHz**

In Figure 5.3, the measurement of the output 1dB compression point yields a +26.9dBm compared to the 26.5dBm given in the datasheet of the amplifier [40].

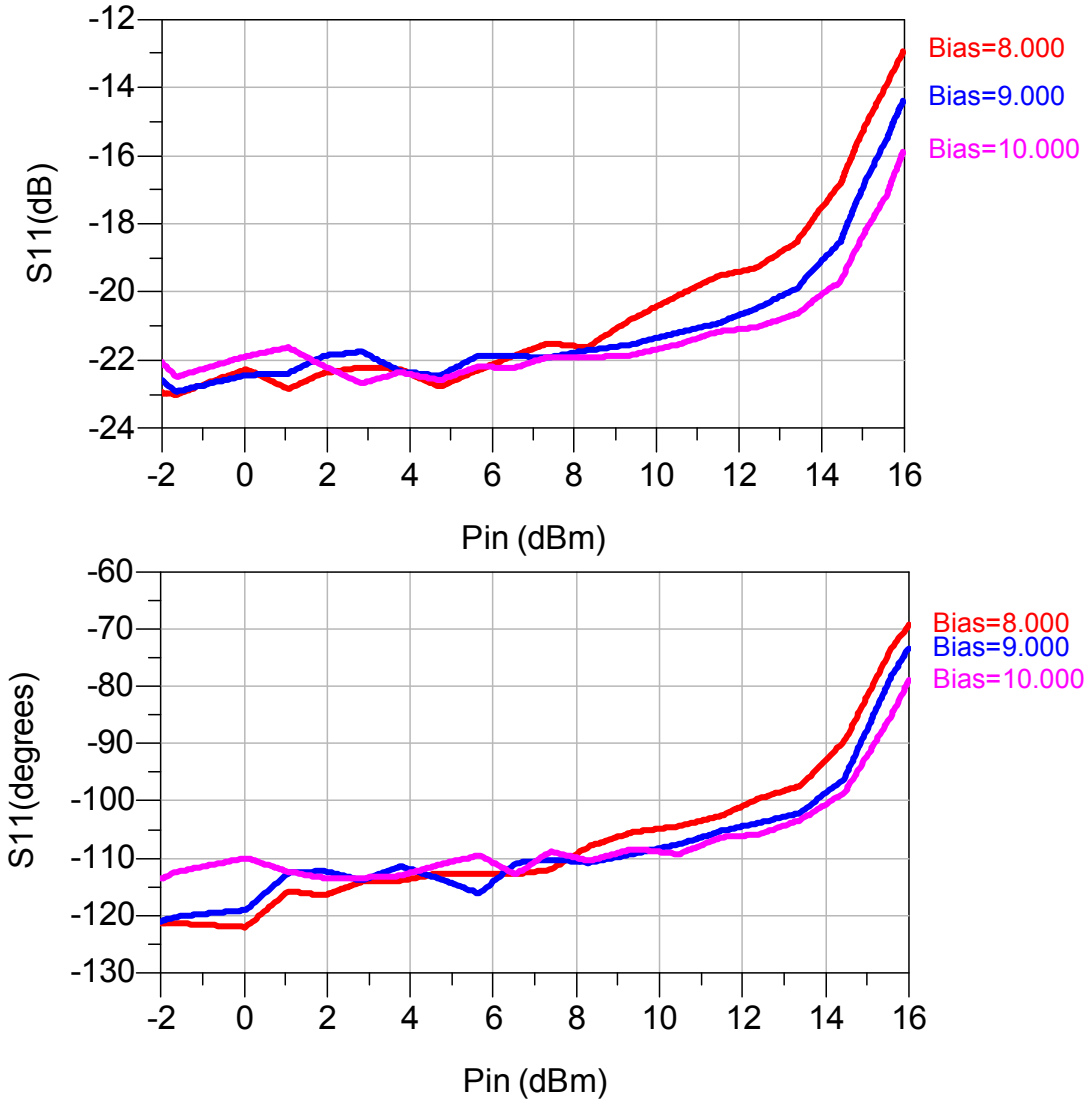


**Figure 5.4 – $S_{11}$ vs. Power Response of the AH101 Amplifier at 900MHz**

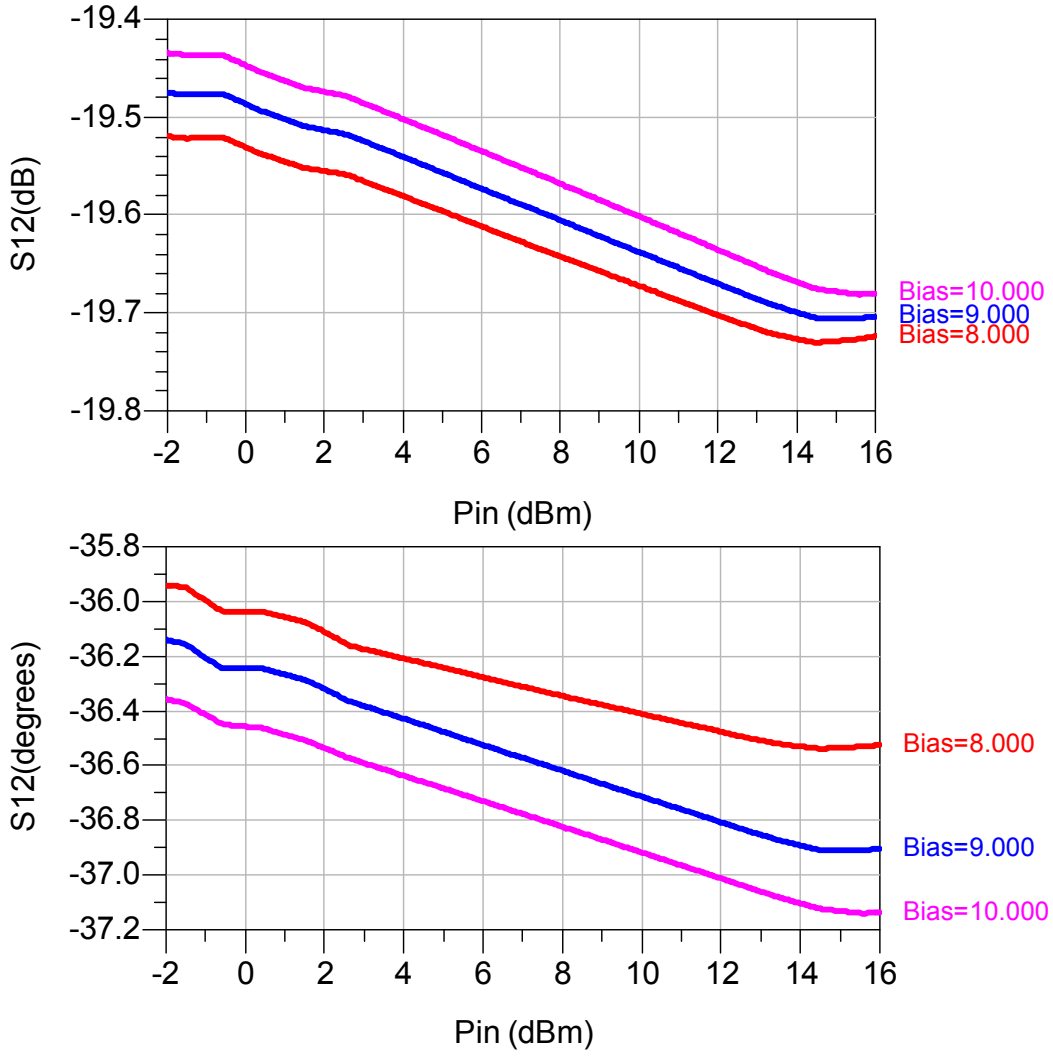


**Figure 5.5 – $S_{12}$ vs. Port 2 Power Response of the AH101 Amplifier at 900MHz**

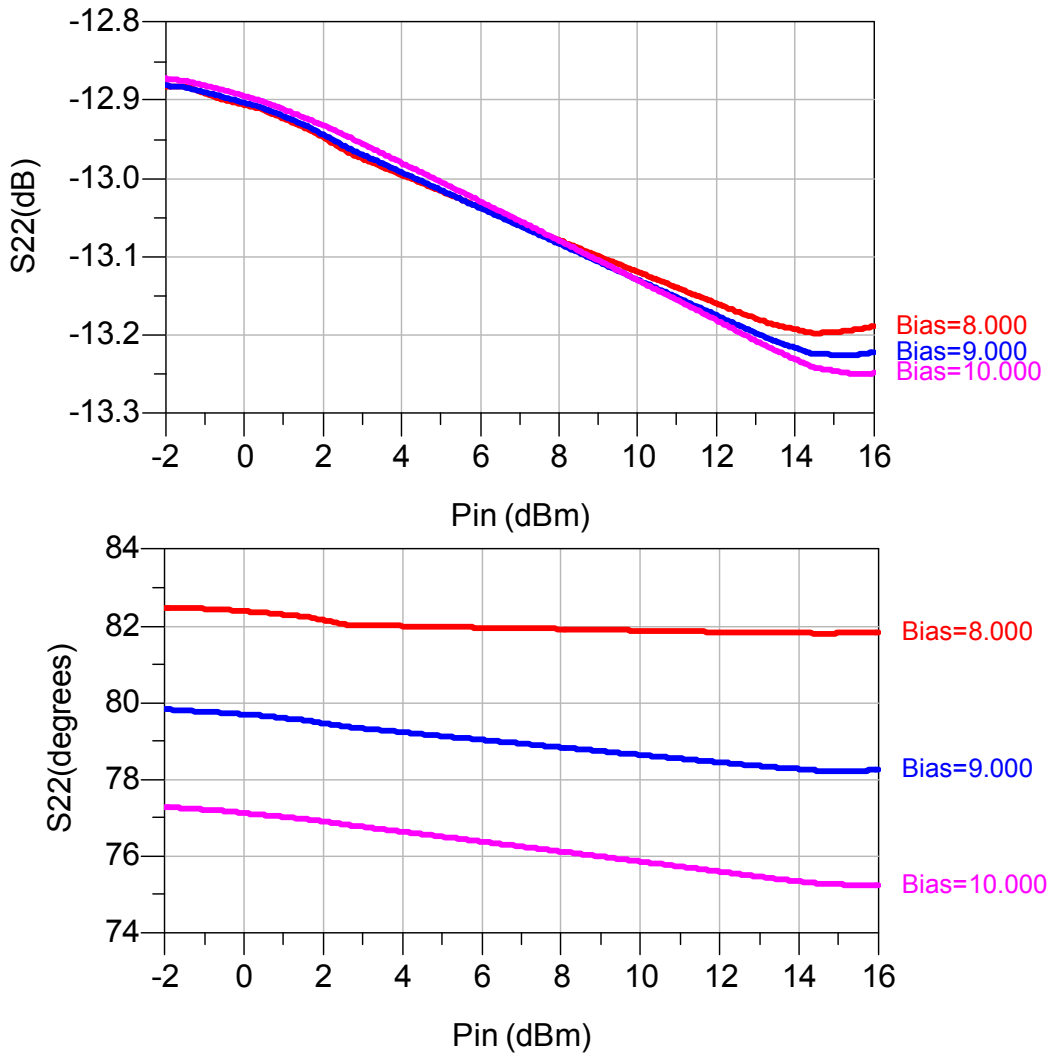


**Figure 5.6 – S22 vs. Port 2 Power Response of the AH101 Amplifier at 900MHz**

The S2D model was also generated and it will be tested in ADS using the circuit schematic presented on Figure 5.7.

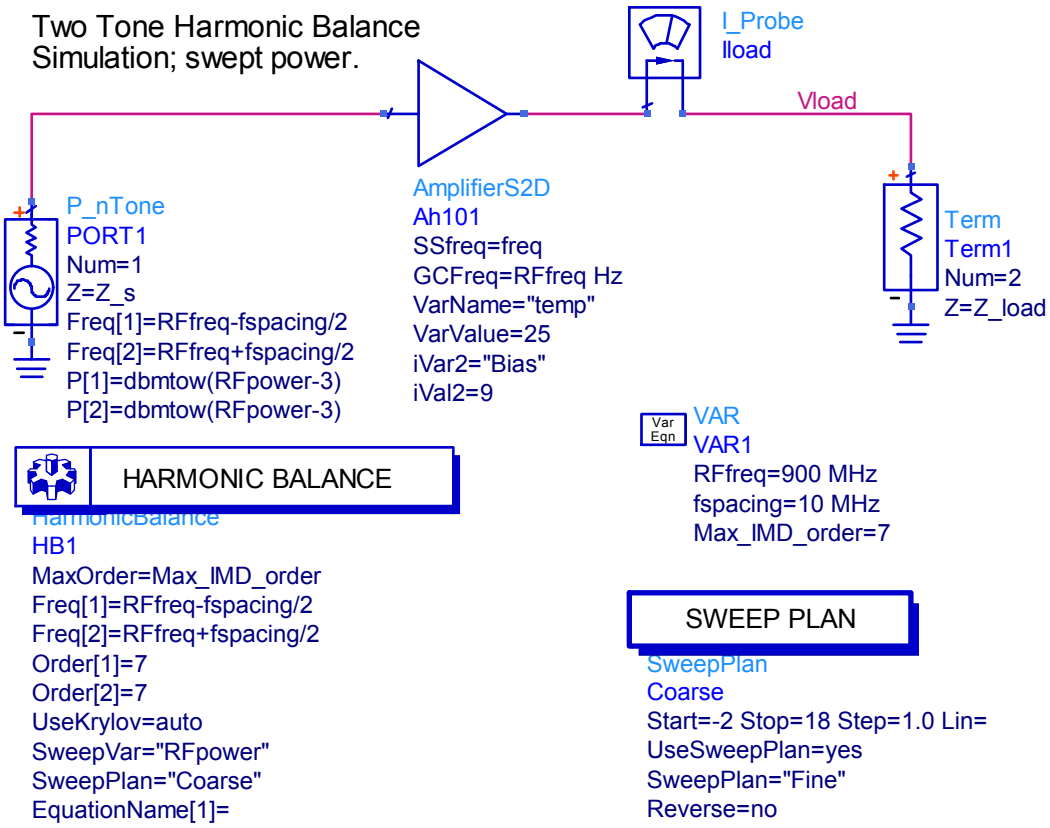


**Figure 5.7 – Circuit Schematic Used to Simulate an S2D Model.**

The main feature of an S2D model is its ability to predict odd order harmonics and odd order intermodulation products. The simulation was performed with a two tone excitation with a separation of 10MHz. The simulated bias condition was 9 volts the output power for both tones was set to 8dBm. The results obtained from this simulation are plotted in Figure 5.8.

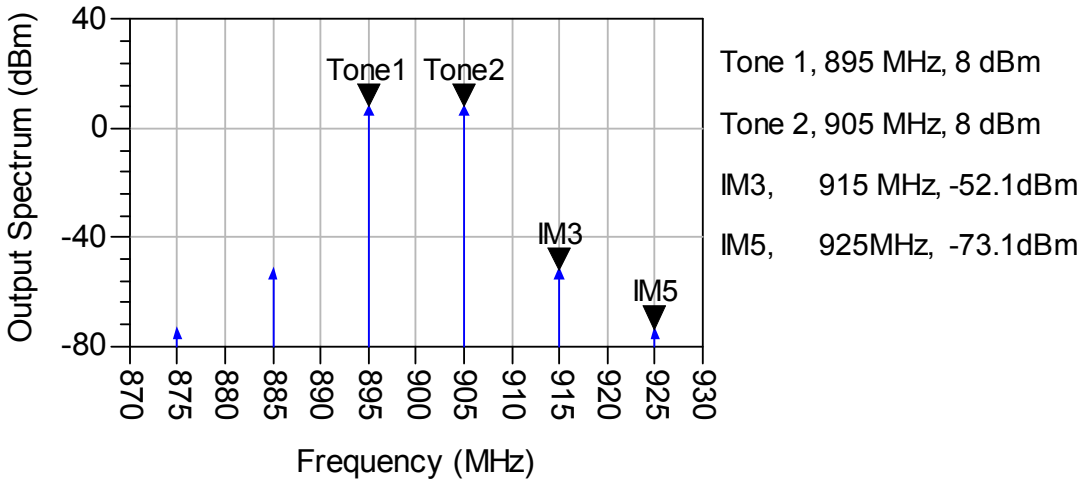


**Figure 5.8 – Output Spectrum of the Simulated S2D Model for an Output Power of 8dBm/Tone.**

### 5.3 Time Budget

Since the purpose of this thesis was to develop more efficient ways to perform the measurements and generate the models, it will be interesting to do a quantification of the time spent during the measurements. The same approach used on section 4.3 will be used here. Table 5.2 summarizes the conditions under which the device was modeled. In table 5.3, estimations the time that would be required to perform these measurements manually are given for comparison.

**Table 5.3 – Quantification and Time Estimation for the Proposed Amplifier**

| Meas. Type | Quantification | Estimated Time |
|---|---|---|
| VNA DUT Measurements | 3(Bias)x3(samples)x(1(freq.S)+22(pow.S)) =207 Swept Meas. | ~ 8 hours 2 min. avg. per measurement (incl. manual adjustments and 1 min per connection) |
| | 69 Connections / Probings | |
| | 207 Manual adjustments of Bias and VNA configuration. | |
| SOLT Calibrations | 4(SOLT)x(1(freq.S)+22(Pow.S.)))= 92 Connections / 92 Swept Meas. | 23 calibrations taking: ~ 4.6 hours |

After performing the measurements with the automation procedures and the generated code we obtained the following measurement times.

**Table 5.4 – Actual Measurement Time Obtained with the Code**

| Measurement Type | Time |
|---|---|
| DUT | 1 hour 57 minutes |
| Calibration standards | 19 minutes |

Based on the time estimations of Table 5.3 (756 minutes) and the actual time spent in the measurement of Table 5.4 (136 minutes), a time efficiency of 556% was achieved with the automated code.

## 5.4 Conclusions

The methodologies developed in Chapter 4 for generating measurement based behavioral models were demonstrated with a commercial amplifier. The automation through the use of LabVIEW code yielded a 556% time efficiency improvement over a manual measurement. The models generated were capable of predicting well the behavior of the amplifier as specified in the datasheet.

# CHAPTER 6

# SUMMARY AND RECOMMENDATIONS FOR FUTURE WORK

## 6.1 Summary

This thesis presented a study and implementation of a methodology to extract measurement based behavioral models with classical Vector Network Analyzers (VNAs). All the procedures and techniques were implemented as several NI LabVIEW applications that will control the measurement instrumentation to efficiently generate the models.

The capabilities of classical VNAs to capture non-linear behavior are generally limited to power dependent S-Parameters that can be extracted with a power sweep. For the types of behavioral models treated in this work, multiple power sweeps at different frequencies combined with regular frequency sweep S-Parameters must be measured under all the modeling conditions implying a multitude of measurements. Connections and calibrations were identified as the elements in the procedure requiring more time. Automation was the solution provided to minimize the total number of connections required for measuring both DUT and calibration standards. This automation will make the code to set the all the required configurations in the VNA and obtain frequency and power dependent S-Parameter data every time a connection is made. The second step taken towards an efficient generation of the models was to minimize the effort required

for calibration. A study of the available network analyzers concluded with a set of conditions that must be met in order to minimize the measurements required for calibration. These conditions established that if compression in the samplers of the VNA is avoided and no change in the internal attenuation settings of the VNA is required the error terms obtained from a calibration will stay constant with power. Sampler compression needs to be avoided with careful design of the measurement setup. In addition, knowledge of the VNA internal structure will determine the minimum number of measurements of the calibration standards required to achieve calibration.

The previous analysis was performed for the Agilent HP87XX Series and the Anritsu Lightning Series network analyzers. Based on these two network analyzers code was implemented to automate the power and frequency swept measurement process. The user inputs the measurement configurations to use in the VNA and the code finds the most efficient approach to perform the calibrations. Additional considerations include obtaining a reference for absolute power as the input levels driven into the DUT need to be known in order to generate the model. The error terms computed as a result from the calibrations are stored locally in an external computer.

A second application was implemented to sequence the measurements on the DUT. This application will use the previously obtained calibrations and apply them to the VNA to obtain frequency and power sweep S-Parameter measurements. This application is capable also to control instrumentation to set the modeling conditions associated with biasing. All the data obtained from the DUT is stored in a convenient format to later generate the models.

A final application takes all the DUT measurements and puts them into the appropriate syntaxes required by the simulator. The syntaxes for P2D and S2D models were implemented as an example for this thesis. An extra step to convert multiple frequency sweeps at different power levels to a power sweep was required for the Anritsu Lightning since this analyzer does not support vector correction while in power sweep mode.

All the developed code and procedures were tested with commercial amplifiers showing total time efficiency improvement of 500% percent in one case.

### 6.2 Recommendations

All the work presented on this thesis is centered on the network analyzer as principal measurement instrumentation. Additional instrumentation can be introduced into the measurement setup to capture effects that a VNA cannot. With the help of a spectrum analyzer information of even order harmonics generated by the device can be extracted as only odd order harmonics can be predicted from a compression curve. Alternative behavioral models can utilize this information for enhanced second order distortion prediction.

Non-linear measurements based on power sweep have an important limitation when measuring S12 and S22 S-Parameter data. As the signal used for obtaining the ratios used for the S-Parameters will be sweeping at the output port of the DUT and no signal will be fed at the input, the significance of the obtained S22 and S12 is questionable. A different methodology known as HOT S-Parameters that uses a constant tone at the input generated with an external source combined with the excitation

generated by the VNA can provide information on stability, output match or even memory effects. Chapter 3 discussed some of the advantages of this type of measurements and a preliminary attempt of this type of measurement is presented on Appendix A.

Additional considerations can be made in terms of how the reference for absolute power is taken. An external power meter has been used through this work to measure the actual power values inputted to the DUT. However, the input reflection presented by the DUT, may differ from that of the power meter. Corrections where performed to compute the actual power driven into the DUT based on the measured input reflection coefficient. However, further work will be required to study the effects of input and output match and how they interact with the power level that sets the operating point (e.g. small signal, large signal) of the amplifier.

Although only S2D and P2D models were used in this work; additional models can be generated as only the last application will be needed to be updated. Some of typical parametric models can be easily generated from the data obtained as they are usually based on gain compression characteristics (e.g. 1dB compression point or IP3, and IP2). Other more advanced models can be generated with additional instrumentation like the simplified PHD model proposed by Liu in [6] that requires a tuning load at the output.

Finally, with a non-linear VNA the more advanced and complete X-Parameter/PHD models can be generated. Such models treat even as well as odd order non-linearities. Because phase information is included for multiple harmonics with the X-

Parameter approach improved prediction of non-linearities in cascaded components becomes possible as well as the conversion to time domain to enable waveform analyses.

## REFERENCES


[1] J. Wood, " Volterra Methods for Behavioral Modeling," in Fundamentals of Nonlinear Behavioral Modeling for RF and Microwave Design, J. Wood, D.E. Root Ed. Norwood: Artech House, Inc., 2005, pp. 9-36.

[2] Advanced Design System 2006 from Agilent Technologies, inc., CA, USA, www.agilent.com.

[3] Wood, J.; Qin, X.; Cognata, A. "Nonlinear microwave/RF system design and simulation using Agilent ADS 'system - data models" Behavioral Modeling and Simulation, 2002. BMAS 2002. Proceedings of the 2002 IEEE International Workshop on 6-8 Oct. 2002 Page(s):75-79.

[4] Advanced Design System 2006 from Agilent Technologies, inc., CA, USA, www.agilent.com.

[5] Verspecht, J., Root, D.E., "Polyharmonic Distortion Modeling" IEEE Microwave Magazine, June 2006, p.44-57.

[6] Jiang Liu; Dunleavy, L.P.; Arslan, H., "Large-signal behavioral modeling of nonlinear amplifiers based on load-pull AM-AM and AM-PM measurements," Microwave Theory and Techniques, IEEE Transactions on , vol.54, no.8, pp.3191-3196, Aug. 2006.

[7] Steve C. Cripps, "RF Power Amplifiers for Wireless Communications," 2nd ed. , Norwood: Artech House, 2006.

[8] Ku, H., McKinley, M.D., Kenney, J.S., "Quantifying Memory Effects in RF Power Amplifiers" IEEE Transactions on Microwave Theory and Techniques. Vol. 50, No. 12, December 2002.

[9] P.M. Cabral, J.C. Pedro, N.B. Carvalho, "Modeling nonlinear memory effects on the AM/AM, AM/PM and two-tone IMD in microwave PA circuits," International Journal of RF and Microwave Computer-Aided Engineering, vol. 16, no. 1, pp. 13-23, Jan., 2006.

[10] Steve C. Cripps, "Advanced Techniques in RF Power Amplifier Design," Norwoodf: Artech House, 2002.

[11] Maas, S.A. “Nonlinear Microwave circuits” Artech House Publishers 2nd Edition 2003.

[12] Pedro, J. C. and Maas, S. A., "A comparative overview of microwave and wireless power-amplifier behavioral modeling approaches," Microwave Theory and Techniques, IEEE Transactions on, vol. 53, no. 4, pp.1150-1163, 2005.

[13] A. Zhu, and T. J. Brazil, “An Overview of Volterra Series Based Behavioral Modeling of RF/Microwave Power Amplifiers (Invited)”, The 8th annual IEEE Wireless and Microwave Technology (WAMICON) Conference, Clearwater, FL, Dec. 2006.

[14] R. B. Marks and D. F. Williams, “A general waveguide circuit theory,” J. Res. Natl. Inst. Stand. Technol., vol. 97, no. 5, pp. 533–562, Sept.-Oct. 1992.

[15] Verspecht, J., Bossche, M.V., and Verbeyst, F., “Characterizing Components Under Large Signal Excitation: Defining Sensible “Large Signal S-Parameters”?!” 49th ARFTG Conference Digest. Spring 1997.

[16] D. E. Root, J. Verspecht, D. Sharrit, J. Wood, and A. Cognata, “Broad-band poly-harmonic distortion (PHD) behavioral models from fast automated simulations and large-signal vectorial network measurements,” IEEE Trans. Microw. Theory Tech., vol. 53, no. 11, pp. 3656–3664, Nov. 2005.

[17] Verspecht, J., Williams, D.F., Schreurs, D., Remley, K.A., McKinley, M.D., “Linearization of Large-Signal Scattering Functions” IEEE Transactions on Microwave Theory and Techniques. Vol. 53, No. 4, April 2005.

[18] S. Maas, Microwave Mixers, Second Edition, Artech House, Norwood, MA, 1993.

[19] Williams, D.F., Ndagijimana, F., Remley, K.A., Dunsmore, J.A., Hubert, S., “Scattering-Parameter Models and Representations for Microwave Mixers” IEEE Transactions on Microwave Theory and Techniques. Vol. 53, No. 1, January 2005.

[20] Verspecht, J., "Large-signal network analysis," Microwave Magazine, IEEE , vol.6, no.4, pp. 82-92, Dec 2005

[21] Model 372XXC/373XXC Vector Network Analyzer Maintenance Manual, Anritsu Corporation, Morgan Hill, CA, 2004.

[22] J. Fitzpatrick, “Error models for system measurements,” Microwave J., vol. 21, no. 5, pp. 63-66, May 1978.

[23] S. Padmanabhan, L. Dunleavy, J.E. Daniel, A. Rodriguez, and P.L. Kirby, “Broadband Space Conservative On-Wafer Network Analyzer Calibrations with More Complex Load and Thru Models.” IEEE vol.54 no.9, September, 2006. pp.3583-3593.

[24] A. Ferrero and U. Pisani, “Two-port network analyzer calibration using and unknown “thru”,” Microwave and Guided Wave Letters, pp. 505-507, 1992.

[25] J.E. Daniel, “Development Of Enhanced Multiport Network Analyzer Calibrations Using Non-Ideal Standards,” M.S. thesis, EE Dept., USF, Tampa, FL, 2005.

[26] H. J. Eul and B. Schiek, “Thru-match-reflect: One result of a rigorous theory for de-embedding and network analyzer calibration,” in Proc. 18th European Microwave Conf., Stockholm, Sweden, Sept. 1988, pp. 909-914.

[27] R. Marks, “A multiline method of network analyzer calibration,” IEEE Microwave Theory and Tech., vol. 39, pp. 1205-1215, July 1991.

[28] A. Davidson. E. Strid. and K. Jones “Achieving greater on-wafer S-parameter accuracy with the LRM calibration technique.” IEEE ARFTG Digest Dec. 1989.

[29] Doug Rytting, “Network Analyzer Error Models and Calibration Methods,” 54th ARFTG Conference short notes, December 2000.

[30] National Instruments Corporation, LabVIEW™, 11500 N Mopac Expwy, Austin, TX 78759.

[31] D. Sosa-Martin, L.P. Dunleavy. (2009, January) Program Calibrates VNA for Broadband Accuracy. Microwaves & RF. Available: http://www.mwrf.com/Articles/ArticleID/20585/20585.html

[32] “Hot S22 and hot K-factor measurements,” Morgan Hill, CA: Anritsu, Applicat. Note (Scorpion), July 2002.

[33] G. Collinson and M. Jones, “A novel technique for measuring small signal S-parameters of an RF/microwave, transistor power amplifying stage for use in power amplifier stability analysis,” in IEEE MTT-S Int. Microwave Symp. Dig., 1993, pp. 1255-1258.

[34] Tony Gasseling, Denis Barataud, Sébastien Mons, Jean-Michel Nébus, Jean-Pierre Villotte, Juan J. Obregon and Raymond Quéré,”Hot Small-Signal S-parameter Measurements of Power Transistors Operating Under Large-Signal Conditions in a Load-Pull Environment for the Study of Nonlinear Parametric Interactions,” IEEE Transactions on Microwave Theory and Techniques, Vol.52, No.3, March 2004.

[35] Cabral, P.M.; Pedro, J.C.; Carvalho, N.B., "Dynamic AM-AM and AM-PM behavior in microwave PA circuits," Microwave Conference Proceedings, 2005. APMC 2005. Asia-Pacific Conference Proceedings , vol.4, no., pp. 4 pp.-, 4-7 Dec. 2005.

[36] J. Martens and P. Kapetanic, “Probe-tone S-parameter measurements,” IEEE Trans. Microwave Theory Tech., vol. 50, pp. 2076-2082, Sept. 2002.

[37] L.P. Dunleavy, J. Liu. (2007, July) Understanding P2D Nonlinear Models. Microwaves & RF. Available: http://www.mwrf.com/Article/ArticleID/16043/16043.html.

[38] J. Martens, “On quantifying the effects of receiver linearity on VNA calibrations,” presented at the 70th Automatic RF Techniques Group. High Power RF Measurement Techniques, Tempe, AZ, 2007.

[39] R. B. Marks, J. A. Jargon, John R. Juroshek, “Calibration Comparison Method for Vector Network Analyzers,” 48th ARFTG Conf. Digest, pp 38-45, Dec 5-6 1996.

[40] TriQuint Semiconductor, “AH101 Medium Power, High Linearity Amplifier,” AH101 datasheet, May. 2009.

[41] S. Kenney, "Nonlinear Microwave Measurements and Characterization," in Commercial Wireless Circuits and Components Handbook, J.M. Golio Ed. Boca Raton: CRC Press LLC, 2003, pp. 16.1-16.21.

**APPENDICES**

## Appendix A: Hot S-Parameter Setup

In this appendix a proposal to obtain HOT S-Parameter measurements is presented as it enables to obtain additional information from the DUT. These types of measurements were theoretically introduced on Chapter 3, and a preliminary approach to obtain them including some demonstration is presented here.

### A.1 HOT S-Parameter Measurement Setup

The measurement setup used is similar to that used by Martens and Kapetanic on [36], with the introduction of some capabilities like the sweeping of the driving tone (high power) with the probe tone (VNA test signal.) LabVIEW™ code was implemented to automate the needed measurements.

The measurement setup was built with the following instrumentation:

- Anritsu 37XXX Lightning VNA.
- Anritsu 68067 CW Generator used to generate the probe tone.
- The Agilent HP87XX Series was also used but it does not support all the capabilities implemented in the code. Unless indicated otherwise, all the procedures presented below were developed for the Anritsu Lighting.

The Anritsu Lightning will generate the probe tone and measure S-Parameters, while the RF generator will generate a CW high power tone that will be kept constantly connected to the input of the DUT. The setup used for this measurement is presented on figure A.1.

**Appendix A (Continued)**

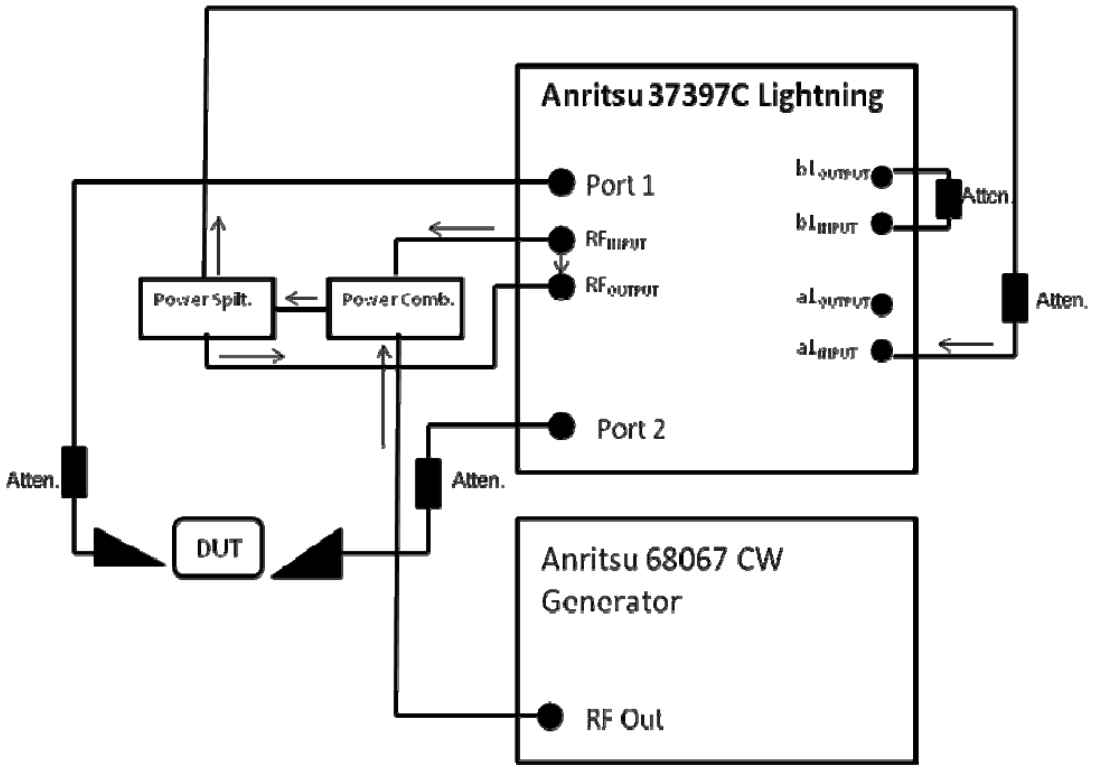


**Figure A.1 – HOT S-Parameters Measurement Setup with RF Insertion**

The previous setup combines the probe tone from the VNA and the driving tone from the external RF generator and inserts it back to the VNA. The RF insertion method is implemented as it was tested to present a better stability in the Automatic Leveling Control (ALC) of the VNA. Although in [36] the same structure was implemented, the reasons were different. Martens used modulated signal that will share bandwidth with the probe tone and, therefore, its effect in the S-Parameter measurement will be ratioed out as it was present in both samplers. In our setup, a single frequency continuous wave tone was used with the condition that it must be outside the IF bandwidth of the VNA to avoid disturbance of its phase lock system.

**Appendix A (Continued)**

An initial consideration for the measurement will be the frequency of the driving tone. It would be desirable to use a driving tone frequency as close as possible to the probe tone so the measurement in the VNA captures the actual frequency response of the DUT. However, the driving tone has to be outside of the IF bandwidth the VNA is configured to, otherwise the measurement will be disturbed. It will be described later; the implemented applications allow sweeping the frequency of the driving tone keeping a constant distance with the probe tone.

A second consideration will be the appropriate difference in power between probe and driving tones. The probe tone should be low enough so it does not produce a significant change in the linearity of the device. This means that the grade of non-linear behavior of the DUT should be set exclusively by the driving tone. On the other hand, a low power from the probe tone can reduce the accuracy of the measurement and generate errors with the ALC of the network analyzer.

At the time of setting the configuration of the VNA, the two previous considerations must be taken into account. Although no definite rule was found for frequency and power difference between probe and driving tone, a combination of 10dB and 4MHz were values that gave good results. In most of the cases, these values will need to be tuned for the particular measurement setup.

**Appendix A (Continued)**

**A.2 Code for Automation**

From the previous analysis the following tasks were identified for automation:

- The frequency of the driving tone needs to be swept to keep a constant frequency difference with the probe tone.
- An interesting effect to observe is the change in the HOT S-Parameters with increasing power of the driving tone. For this multiple measurements with different power levels will be required. The result will be multiple HOT S-parameter measurements that could be converted to power sweep measurements following the same procedure explained on section 4.8.
- As the purpose is to characterize non-linear behavior, it is important to know the absolute power level going into the device. Therefore, all the combinations excitations with frequency and power inputted to the DUT need to be measured with the power meter.

The three tasks have been implemented in a LabVIEW application whose functionality is presented below.

## Appendix A (Continued)

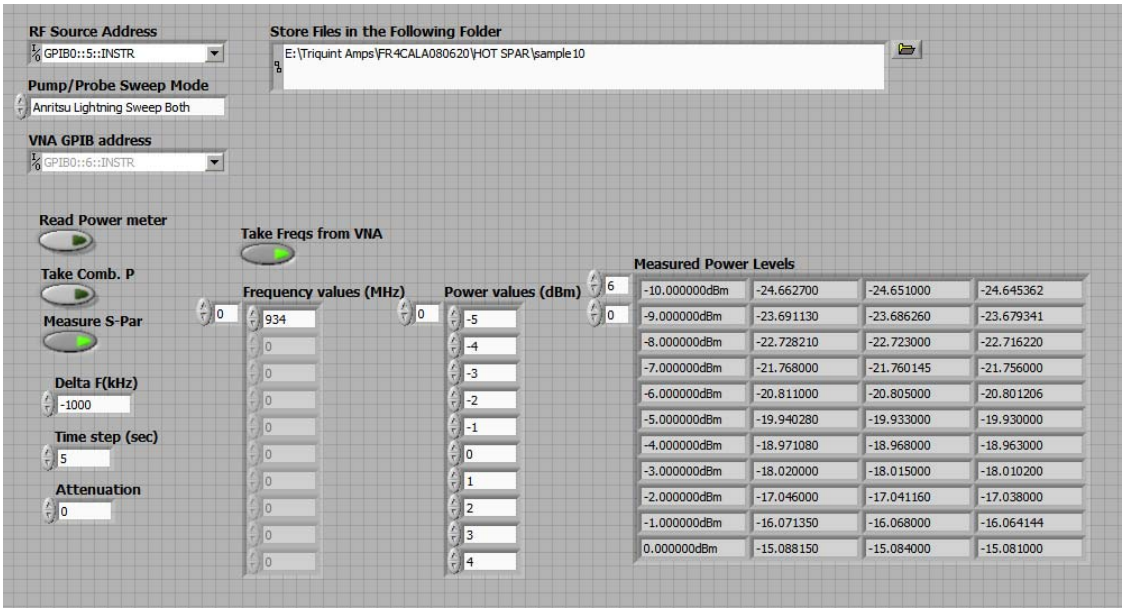


**Figure A.2 – Application that Automates the HOT S-Parameters Measurement**

On figure A.2, the user's interface of the application that automates the measurements needed for HOT S-parameter is shown. It can be distinguished several options that allow either sweeping both (probe and driving tones) or setting the driving tone to a fixed frequency. When the frequency of the driving tone is fixed, the user will be able to specify the frequencies under which the measurement will be taken. When the driving tone is to be swept with the probe tone, the user will specify the difference in frequency that should be maintained between both tones. Finally, the user can select an option where the excitations are set following the same steps but measurements are taken from the power meter instead of from the VNA. This is necessary for latter mapping S-parameters versus power accurately.

The description of the application in terms of a flow diagram is presented on figure A.3.

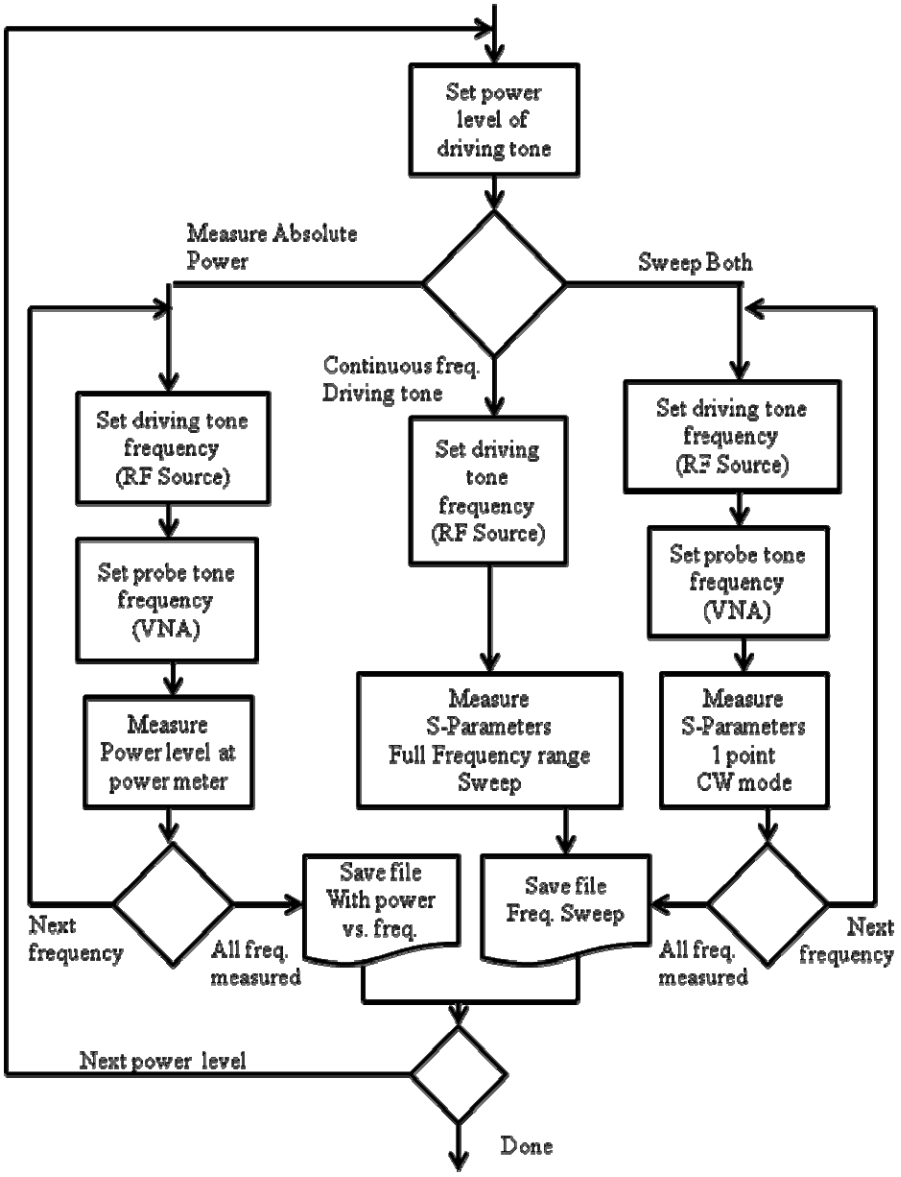


**Figure A.3 – Flow Diagram for HOT S-Parameters Measurements**

## A.3 HOT S-Parameters Measurements

The measurement setup and code proposed was tested with the ZFL-1000LN Mini-Circuits amplifier. The setup used for this is the same than that of Figure A.1 and includes some small modifications that are presented on Figure 5.9.

**Appendix A (Continued)**

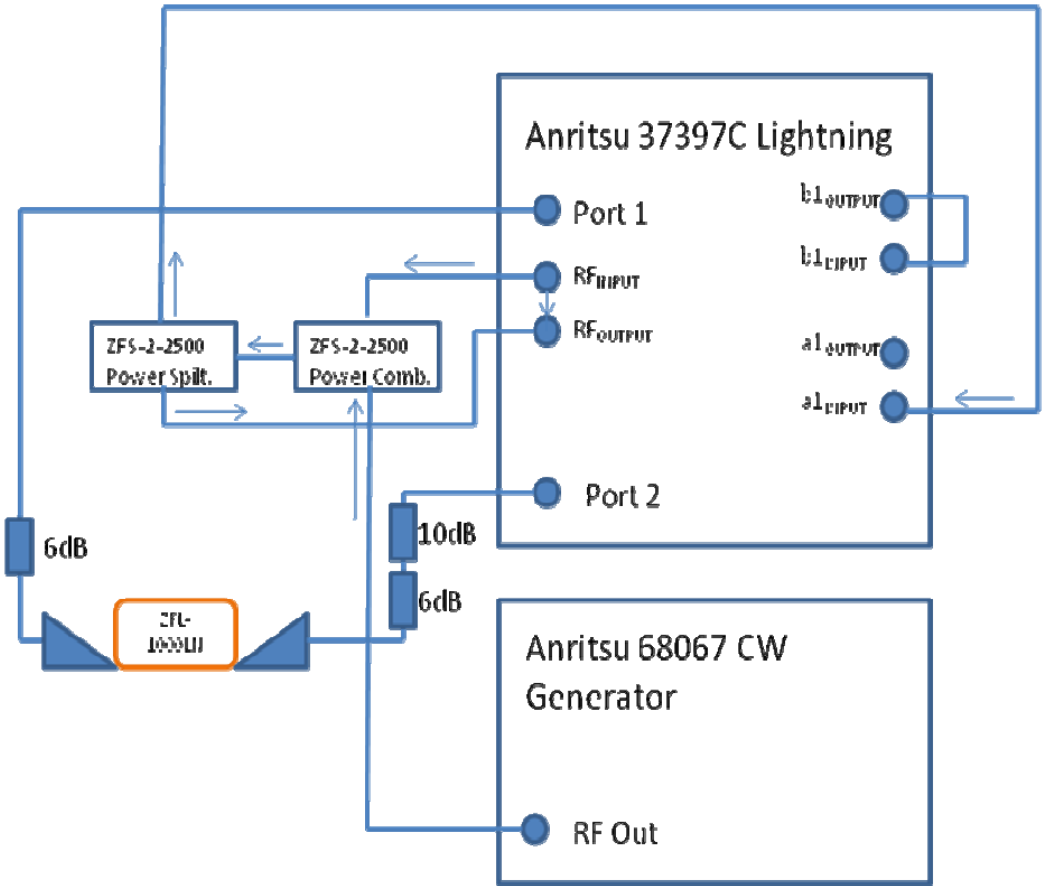


**Figure A.4 – Hot S-parameter Setup Used for Testing the ZFL-1000LN**

With the previous setup the following settings were used:

- Freq. Sweep: 40MHz to 3GHz (51 points.)
- SOLT calibration with Anritsu SMA/3.5mm calibration kit. Isolation included.
- Given that significant attenuation was used to avoid too much power into the sampler. A high average (128) and a low IF bandwidth (10Hz) will recover part of the dynamic range loss with the attenuators.
- The frequency of the driving tone was swept with the probe tone being always 4MHz below the probe's frequency.

**Appendix A (Continued)**

- The power of the driving tone was also swept obtaining input powers on the range from -30dBm to -15dBm.
- All power values were measured with the Anritsu ML2438A.

In order to validate the measurements, regular single tone power swept measurements for $S_{11}$ and $S_{21}$ were compared to HOT S-Parameter measurements with different power levels of the driving tone. The results obtained are presented on Figures A.5 and A.6.

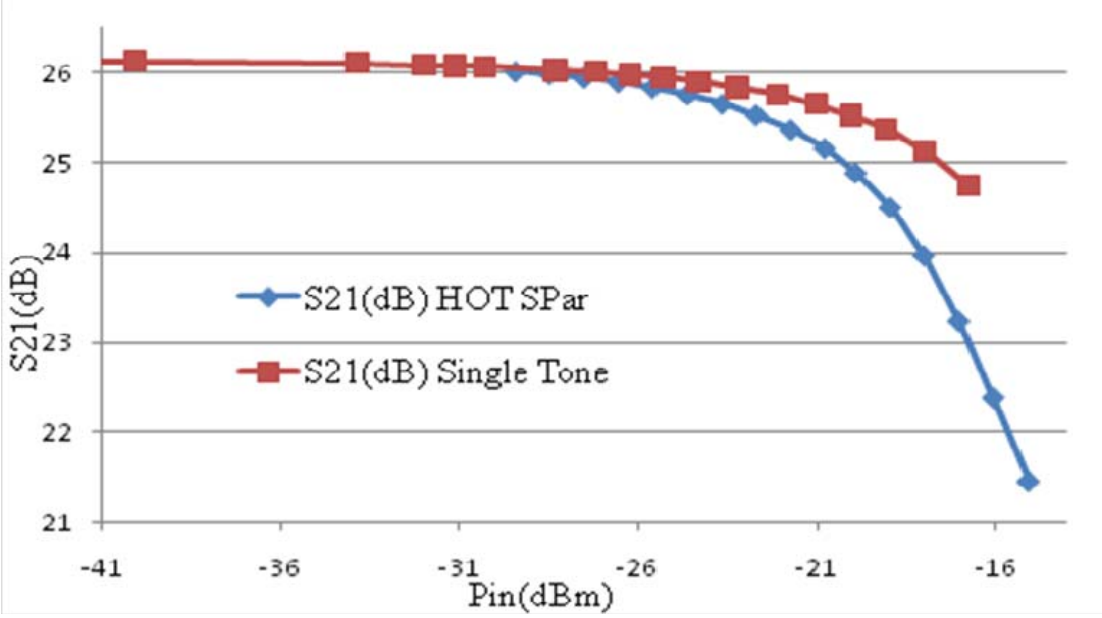


**Figure A.5 – Hot S-Parameter vs. Single Tone Power Sweep. S21 (dB)**

**Appendix A (Continued)**

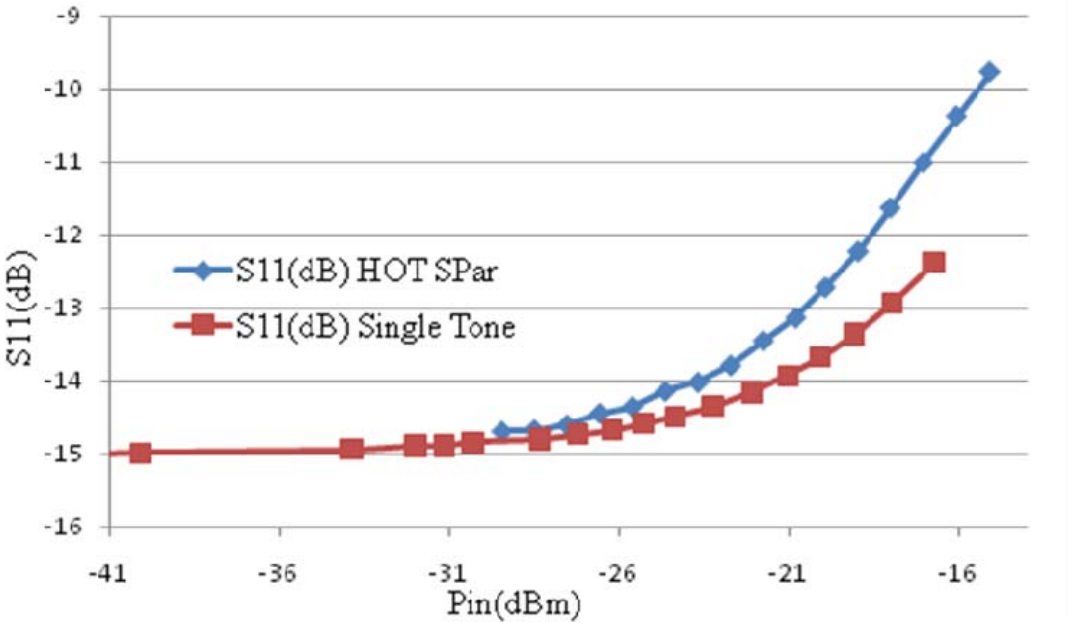


**Figure A.6 – Hot S-parameter vs. Single Tone Power Sweep. S11(dB)**

It can be observed that there is a good agreement in the measurements between HOT S-parameters and single tone power swept S-parameters for S11 and S21 at the lower power levels. The type of validation is being presented here is, to the best knowledge of the author, not present in any of the other attempts of HOT S-parameter measurements available in the literature. Therefore, there is no reference to any possible explanation on some of the differences presented on Figures A.5 and A.6 as power increases. However, some authors (Kenney, [41]) have commented on the inability of single tone power sweep measurements to capture the actual behavior of an amplifier due to the presence of long term memory. Further study should be conducted in order to determine the difference what should be expected from a HOT S-parameter measurement and a single tone power sweep measurement.

**Appendix A (Continued)**

The results obtained for $S_{12}$ and $S_{22}$ are presented on Figures A.7 and A.8 below.

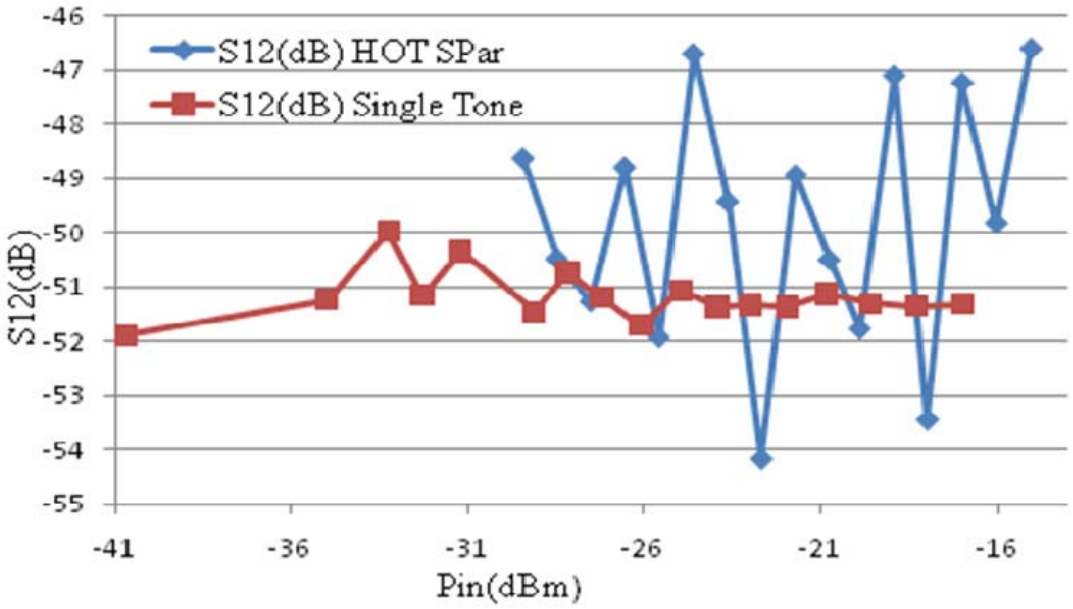


**Figure A.7 – Hot S-Parameter vs. Single Tone Power Sweep. S12 (dB)**

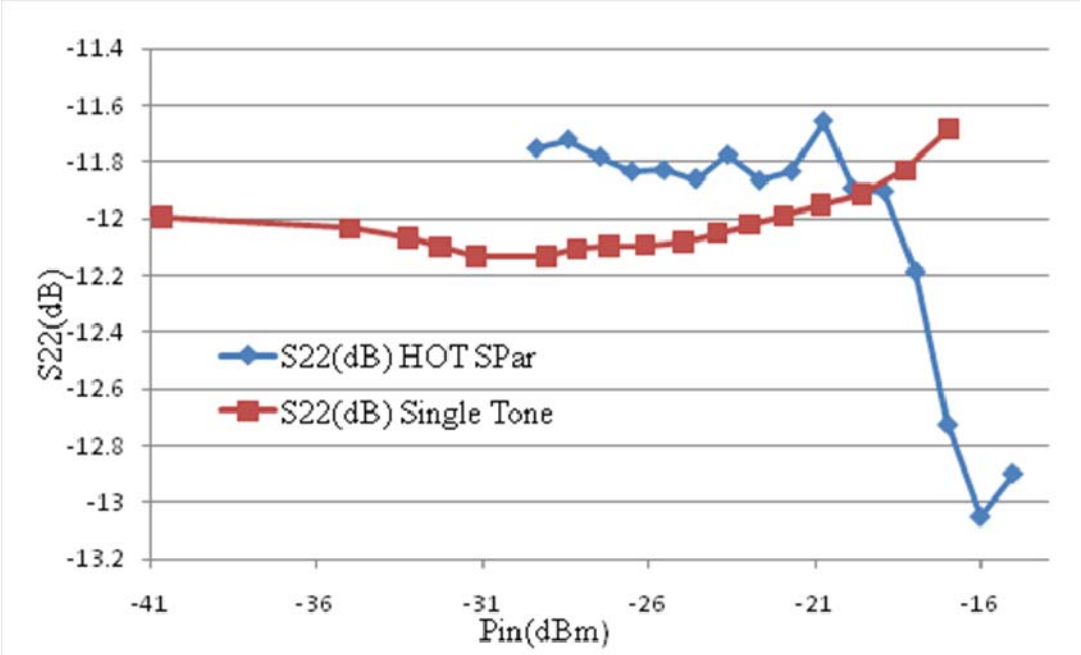


**Figure A.8 – Hot S-Parameter vs. Single Tone Power Sweep. S22 (dB)**

The differences between HOT S-parameter and single tone power sweep are more significant. As it was to be expected, the output match behavior of the device will differ when an input excitation is present at the input than when power is swept only at the output.

## A.4 Conclusion

A setup and a full application to obtain HOT S-parameter measurements with the Anritsu Lightning and an external RF Source (Anritsu 68067) is proposed in this appendix. The setup and code was exemplified with a commercial amplifier and a comparison between the power dependent responses obtain with HOT S-Parameters and single tone power sweep S-Parameters. The previous comparison yielded some differences that will require further research to determine whether they correspond to actual response of the DUT or a particular issue with the measurement setup.